Metal Surface Raman Spectroscopy: Theory

by

R. M. Hexter and M. G. Albrecht

Prepared for Publication

in

Spectrochimica Acta A

University of Minnesota
Department of Chemistry
Minneapolis, MN 55455

March 15, 1978

REPORT DOCUMENTATION PAGE		READ INSTRUCTIONS BEFORE COMPLETING FORM
1. REPORT NUMBER NR 051-642	2. GOVT ACCESSION NO.	3. RECIPIENT'S CATALOG NUMBER
4. TITLE (and Subtitle) Metal Surface Raman Spectroscopy: Theory.		5. TYPE OF REPORT & PERIOD COVERED Technical Report. No. 1
		6. PERFORMING ORG. REPORT NUMBER
7. AUTHOR(s) R. M. /Hexter and M. G. /Albrecht		8. CONTRACT OR GRANT NUMBER(s) N00014-77-C-0209
9. PERFORMING ORGANIZATION NAME AND ADDRESS The Regents of the University of Minnesota Minneapolis, MN 55455		10. PROGRAM ELEMENT, PROJECT, TASK AREA & WORK UNIT NUMBERS
11. CONTROLLING OFFICE NAME AND ADDRESS Chemistry Program Office of Naval Research Arlington, VA 22217		12. REPORT DATE March 15, 1978
		13. NUMBER OF PAGES
14. MONITORING AGENCY NAME & ADDRESS(if different from Controlling Office) TR-1		15. SECURITY CLASS. (of this report) Unclassified
		15a. DECLASSIFICATION/DOWNGRADING SCHEDULE

16. DISTRIBUTION STATEMENT (of this Report)

Approved for public release; distribution unlimited

15 Mar 78

17. DISTRIBUTION STATEMENT (of the abstract entered in Block 20, if different from Report)

76 p.

19. KEY WORDS (Continue on reverse side if necessary and identify by block number)

Surfaces, metal, Raman spectroscopy, surface selection rules, enhanced
Raman intensity of pyridine on silver electrode

20. ABSTRACT (Continue on reverse side if necessary and identify by block number)

Studies of the Raman and infrared spectra of several molecules adsorbed to
metal surfaces indicate that special selection rules govern these spectra. In
the case of infrared reflection adsorption spectroscopy (IRS) as in the related
techniques of electron energy loss spectroscopy (ELS) and inelastic electron
tunneling spectroscopy (IETS), only modes which develop dipole moment perpen-
dicular to the metal surface can be excited. We have shown that an image field

DD FORM 1473 EDITION OF 1 NOV 65 IS OBSOLETE
S/N 0102-014-6601

233 515

EB

model which has been proposed to account for these observations is equivalent to the presence of a new symmetry operation which consists of <u>simultaneous</u> reflection in the plane of the metal surface plus charge conjugation. As a result, instead of the point group of the molecule, the symmetry group which should be used to analyze the motions of a molecule adsorbed to a metal surface consists of the direct product group of the molecular point group and another which is isomorphous with C_2. Furthermore, the activity representations of the system, molecule + image, for both infrared and Raman spectra, are those which are compatible with the totally symmetric representation of C_2.

Both infrared and Raman spectra of oriented metal adsorbates can therefore be used to probe molecular orientation. Depolarization ratios for specific orientations and scattering geometries have been derived and used to analyze the results of several experimental examples. The adsorbed molecule whose Raman spectrum has been most thoroughly studied is pyridine on silver. Using secondary ion mass spectroscopy, we have been able to show that the silver surfaces are atomically quite clean.

The case of pyridine adsorbed on Ag is also of interest because of the relative intensity of some of its Raman lines. By comparison with the same lines in liquid pyridine, the intensity is apparently enhanced by a factor of 10^4. Several theories of this enhancement are analyzed, including the possibility that the enhancement is a demonstration of the resonance Raman effect in which the surface plasmons mix with molecular electronicstates so as to form a <u>continuum</u> of intermediate states for the scattering. Each theory implies a particular dependence of the Raman intensity on the frequency of the exciting radiation. Resonance interaction with the surface plasmons gives the closest agreement with experimental results.

Metal Surface Raman Spectroscopy: Theory

R. M. Hexter and M. G. Albrecht
Department of Chemistry
University of Minnesota
Minneapolis, MN 55455

ABSTRACT

Studies of the Raman and infrared spectra of several molecules adsorbed to metal surfaces indicate that special selection rules govern these spectra. In the case of infrared reflection adsorption spectroscopy (IRS) as in the related techniques of electron energy loss spectroscopy (ELS) and inelastic electron tunneling spectroscopy (IETS), only modes which develop dipole moment perpendicular to the metal surface can be excited. We have shown that an image field model which has been proposed to account for these observations is equivalent to the presence of a new symmetry operation which consists of simultaneous reflection in the plane of the metal surface plus charge conjugation. As a result, instead of the point group of the molecule, the symmetry group which should be used to analyze the motions of a molecule adsorbed to a metal surface consists of the direct product group of the molecular point group and another which is isomorphous with C_2. Furthermore, the activity representations of the system, molecule + image, for both infrared and Raman spectra, are those which are compatible with the totally symmetric representation of C_2.

Both infrared and Raman spectra of oriented metal adsorbates can therefore be used to probe molecular orientation. Depolarization ratios for specific orientations and scattering geometries have been derived and used to analyze the results of several experimental examples. The adsorbed molecule whose Raman spectrum has been most thoroughly studied is pyridine on silver. Using secondary ion mass spectroscopy, we have been able to show that the silver surfaces are atomically quite clean.

The case of pyridine adsorbed on Ag is also of interest because of the relative intensity of some of its Raman lines. By comparison with the same lines in liquid pyridine, the intensity is apparently enhanced by a factor of 10^4. Several theories of this enhancement are analyzed, including the possibility that the enhancement is a demonstration of the resonance Raman effect in which the surface plasmons mix with molecular electronicstates so as to form a continuum of intermediate states for the scattering. Each theory implies a particular dependence of the Raman intensity on the frequency of the exciting radiation. Resonance interaction with the surface plasmons gives the closest agreement with experimental results.

Metal Surface Raman Spectroscopy: Theory

R. M. Hexter and M. G. Albrecht
Department of Chemistry
University of Minnesota
Minneapolis, MN 55455

I. INTRODUCTION

Raman spectroscopy of adsorbed molecules on clean metal sur-
faces is a relatively new experimental technique, in contrast to
the related subject of infrared spectroscopy of surfaces, which
has been actively studied since the pioneering investigations by
Terenin[1] and Eischens.[2] Although cross-sections for Raman scatter-
ing are much smaller than those for infrared absorption (e.g.,
10^{-30} cm^2 compared to 10^{-20} cm^2), Raman spectroscopy enjoys the
advantage of quantum detectors, and cw laser excitation of small
samples, such as nanoliter samples of organic liquids, can give
counting rates of $10^4 - 10^5$ sec^{-1}. Indeed, laser experiments
have recently been carried out in which single atoms have been
detected.[3] Moreover, the scattering efficiency of a molecular
system increases by several orders of magnitude when resonance
Raman conditions are satisfied, and by many orders of magnitude
(e.g., $\sim 10^{11}$) when the conditions for coherent anti-Stokes Raman
spectroscopy (CARS) are established. Of special interest to sur-
face physics and chemistry, some recent experimental studies have
suggested the possibility that when a molecule is adsorbed on or
near a metal surface, there may be an enhancement of its Raman
scattering efficiency by a factor of 10^4.

While there has been some prior consideration that selection rules may govern infrared absorption on metal surfaces, there do not appear to have been any similar considerations with respect to Raman scattering. Furthermore, most of the experimental reports of Raman spectra of surfaces have not indicated the role surface excitation waves, or surface plasmons, may play in the stimulation of these spectra. The interaction of electromagnetic radiation with metal surfaces necessarily involves surface plasmons. It is therefore important to appreciate their role in the excitation of electronic excited states on metal surfaces.

It is the purpose of this article to examine the theory of Raman spectroscopy of surfaces, so as to delineate both its power and its limitations. We shall focus our attention on six areas:

1. Surface excitation waves and their detection

2. Optimization of experimental geometry: incidence and scattering angles, polarization and analysis directions

3. Selection rules for infrared and Raman processes on metal surfaces

4. Depolarization of Raman scattering from metal surfaces: The determination of molecular orientation

5.   Experimental Raman and other surface spectroscopic investigations of metal surfaces

6.   Mechanisms for enhancement of Raman intensity by metal surfaces.

Some of these aspects of Raman spectroscopy of metal surfaces were first discussed by Greenler and Slager, and preliminary experimental results were presented.[4] In this article consid-erations Greenler had given earlier to the optimal incident and scattering directions for infrared reflection-absorption spectro-scopy[5] were extended to Raman scattering. The change in excita-tion wavelength was found to make only a modest change in the calculated optimum angle of incidence. The final results were pre-sented only for TM (p or ||) polarization. While this is the only sensible polarization in the infrared, where the real and imaginary parts of the refractive indices of metals are both large, the reduction in magnitude of these parameters at the shorter wave-length used in Raman excitation makes it possible for TE (s or $\perp$) polarization in the visible region to yield useful data. This possibility will be discussed in Section III below in which we shall make use of the more extensive calculations which have been carried out by McIntyre and coworkers, using linear approximation theory.

Of greater concern is the fact that all experimental results reported to date--of either reflection-absorption or of Raman spectra of materials supported on metal surfaces--have been obtained with systems in which the substrates were probably not clean metal surfaces. The Fresnel equations, the solutions to

which yield the optimal incidence angles, as treated either by Greenler or by McIntyre and Aspnes,[6] are for three-phase systems consisting of

      I.   An ambient phase, which is either vacuum, air or possibly a dilute aqueous solution.

     II.   An adsorbed dielectric (the adsorbate).

    III.   A metal substrate.

However, unless the metal is atomically clean prior to the adsorption of the adsorbate, the experimental system has in all likelihood at least four phases, in that it probably has an additional oxide layer in between phases II and III. It may be that this layer has little dielectric consequence (v.i.), but in the absence of evidence to support this possibility, we should at least know its composition and thickness. Because of the current availability of a variety of particle surface spectroscopies, this is now feasible. In a subsequent article we shall report such data.

Within the past year, reports have emanated from a number of laboratories of Raman spectra of pyridine and other amines with greatly enhanced intensities, when these molecules have been adsorbed on silver electrodes following electrochemical cycling of the electrode in an aqueous salt solution containing the dissolved amine. Here, too, the metal surfaces have not been well characterized. Section VI includes data concerning these surfaces.

Nothwithstanding the lack of previous surface characterization studies of the electrodes, the Raman data that have been reported have been interesting, for the observed scattering frequencies have been assigned to particular irreducible representations of the molecular point group, and depolarization ratios for the most intense Raman bands have been reported. A quite approximate calculation of the change in depolarization ratio expected for a change in molecular orientation has also been presented, and in the Section V of the present article this will be compared with more precise calculations.

The foregoing remarks are intended to indicate that our intention is to provide an account of the theory of Raman spectroscopy on metal surfaces that is precise and accurate, that is based upon quantitative physical and spectroscopic principles, and to apply it carefully to the interpretation of the experimental data. Where approximations or assumptions must be made, these will be fully identified, and the extent to which they may affect the results will be evaluated. Throughout the theory will be used as a guide to particular experiments which can enlarge the available data.

II. SURFACE EXCITATION WAVES AND THEIR DETECTION

The purpose of this section is to describe the quanta of surface excitation. These quanta are surface electromagnetic waves, or surface plasmons. The interaction of these waves with light is responsible for certain minima in the reflectance

vs. wavelength curves of metals which we shall discuss later in this section. Although these minima can be observed with smooth metal surfaces, they are significantly modified, both in wavelength and in amplitude, by surface roughness. In studying surface plasmons, we wish to emphasize their wavelike nature, as well as the ways in which they may be coupled with light.

The dispersion relation for electromagnetic radiation is always

$$\omega = \frac{c}{n} k \tag{1}$$

or

$$\omega^2 \varepsilon(\omega) = c^2 k^2 \tag{2}$$

where $n = \varepsilon^{\frac{1}{2}}$ is the refractive index of the medium in which the radiation is propagating.

The complex dielectric response function $\hat{\varepsilon}(\omega)$ of a free electron metal can be shown to be given by

$$\hat{\varepsilon} = 1 - \frac{\omega_p^2}{\omega^2 + i\omega/\tau} \tag{3}$$

where τ is the average time between electron collisions.[7] If we neglect the damping caused by such collisions, Eq. (3) becomes

$$\hat{\varepsilon} \cong 1 - \frac{\omega_p^2}{\omega^2} \tag{4}$$

This function and the dispersion relation for electromagnetic radiation in the medium are illustrated in Fig. 1.

In the region where $\varepsilon < 0$ ($\omega < \omega_p$), the index of refraction of a free electron metal is pure imaginary, and electromagnetic waves cannot be propagated in it. Incident waves are then mostly reflected at its boundary, and the electric field in the medium is attenuated according to $E(z) \sim e^{-|k|z}$. However, in the region $\omega > \omega_p$, the index of refraction is pure real and electromagnetic waves can then be propagated in the metal, according to the dispersion relation illustrated in Fig. 1(b).

The situation is entirely analogous to the more familiar optical modes of an ionic crystal,[8] except that in the free-electron metal, $\omega_t = TO = 0$. The limiting frequency at $\underset{\sim}{k} = 0$ represents a longitudinal mode whose square is given by

$$\omega_p^2 = 4\pi N \underline{e}^2 / \underline{m} \tag{5}$$

where N, $\underline{e}$ and $\underline{m}$ are the density, charge and mass of the electron, respectively. Although ω_p, called the plasma frequency, is the frequency of a longitudinal mode of the bulk metal, this mode is radiative and it can be excited by electromagnetic radiation, provided the electric vector of the light has a component parallel to $\underset{\sim}{k}$, which is normal to the boundary of the metal. On the other hand, it can be seen from the dispersion curve that at $\underset{\sim}{k} = 0$ this mode is not very light-like, so that the dipole strength of the excitation is small. But this does increase with $\underset{\sim}{k}$ and, at the same time, the excitation becomes transverse, like light itself.

Calculation of the reflectance and transmittance of thin metallic films to light that is not normally incident upon them

show that $R_{||}$ and $T_{||}$ will have a maximum and a minimum, respectively, at $\omega = \omega_p$.[9] The resonance at ω_p is favored because the radiative mode at $\omega = \omega_p$ is least damped. Experimental observation of these resonances were first made by McAlister and Stern.[10] Variation of polarization and angle of incidence demonstrates that there is no resonant absorption with s-polarized light, and that $T_{||}$ at $\omega = \omega_p$ decreases with $\sin^2 \phi/\cos \phi$, where ϕ is the angle of incidence (See Sec. III).

We now wish to describe the related excitations of surfaces. There are several types of surfaces which can be discussed, and one or another may correspond to a particular experiment. For example, excitations at the boundary of a metallic slab can be described, or we may wish to study those of a thin metallic film covered on both sides with media of equal dielectric constants.[11] In this case, there are two coupled solutions for the p-polarized electric fields. These are called, respectively, the symmetric (or tangential or tanh) branch and the antisymmetric (or normal or coth) branch. The symmetry notation here refers to the phase relationships between the modes on the two surfaces. The geometric notation refers to the relative polarization of the electric field, and the hyperbolic functions refer to the dependence on $k_{||}$ (k parallel to the surface) in the squared frequency dispersion relation for each mode. We may also wish to consider asymmetric layer systems, which involve three dielectric functions.

Although each of these configurations may be of interest to an experimentalist, there is a simpler configuration that has

within it the essential lessons of all, and we shall concentrate upon this one. This configuration simply consists of the two-phase system, dielectric and metal, with dielectric functions ε_d and ε_m, respectively. The requirement of continuity of the tangential fields at the boundary, $Z = 0$, applied to the solutions to Maxwell's equations for this system[12] yields the dispersion relation

$$k_x = \pm \frac{\omega}{c} \left(\frac{\varepsilon_m \varepsilon_d}{\varepsilon_m + \varepsilon_d} \right)^{\frac{1}{2}} \tag{6}$$

If we now use Eq. (4) for $\varepsilon_m(\omega)$ and assume that $\varepsilon_d(\omega)$ is a constant, the squared frequency dispersion relation becomes

$$\omega^2 = \frac{\omega_p^2 \varepsilon_d + c^2 k_x^2 (1 + \varepsilon_d) \pm \{[\omega_p^2 \varepsilon_d + c^2 k_x^2 (1 + \varepsilon_d)]^2 - 4\omega_p^2 c^2 k_x^2 \varepsilon_d\}^{\frac{1}{2}}}{2\varepsilon_d} \tag{7}$$

Both of these expressions are considerably simplified but retain the same general form if we take $\varepsilon_d \equiv 1$ (i.e., the dielectric is simply a vacuum):

$$k_x = \pm \frac{\omega}{c} \left(\frac{\varepsilon(\omega)}{\varepsilon(\omega) + 1} \right)^{\frac{1}{2}} \tag{8}$$

and:

$$\omega^2 = \tfrac{1}{2}\omega_p^2 + c^2 k_x^2 \pm (\tfrac{1}{4}\omega_p^4 + c^4 k_x^4)^{\frac{1}{2}} \tag{9}$$

Note that the first term of Eq. (9) has the same dependence on k_x as that of the transverse plasmon in a bulk metal. Eq. (9) is illustrated in Fig. 2. The limiting frequency as $k_x \to \infty$ is found

by substituting the condition

$$\varepsilon_m = -\varepsilon_d \tag{10}$$

into Eq. (4), which gives the surface plasma frequency as

$$\omega_s = \frac{\omega_p}{(\varepsilon_d + 1)^{\frac{1}{2}}} \tag{11}$$

or, in the case where the dielectric is a vacuum,

$$\omega_{sp} = \omega_p/\sqrt{2} \tag{12}$$

There is now a closer analogy to the polaritons of an ionic crystal. Propagating solutions of Eq. (8) exist only for frequencies for which $\varepsilon_{1m}(\omega) > 0$ or $\varepsilon_{1m}(\omega) < -\varepsilon_d$. Both branches correspond to transverse modes, except for the limiting frequency ω_p of the first at $k_x = 0$. As in the polariton case, ω_p corresponds to a zero, and the limiting frequency ω_{sp} at $k_x \gg 0$ corresponds to a pole, of the dielectric function. The phase velocity of each branch is given by

$$v_{phase} = \frac{c}{n_d} \left(\frac{\varepsilon_{1m}(\omega) + \varepsilon_d}{\varepsilon_{1m}(\omega)} \right)^{\frac{1}{2}} \tag{13}$$

where $n_d = \varepsilon_d^{\frac{1}{2}}$. Except at $k_x = 0$, the phase velocity in the range $\varepsilon_{1m}(\omega) > 0$ is $v_{phase} > c/n_d$, whereas when $\varepsilon_{1m}(\omega) < -\varepsilon_d$, $v_{phase} < c/n_d$. Hence, the upper branch is radiative but the lower one is non-radiative. In the gap $-\varepsilon_d < \varepsilon_{1m}(\omega) < 0$ there are no surface plasmon modes. We also observe that the dipole strength

of each branch, as in the case of a metal by itself, is greatest where the dispersion relation is most photon-like. In this case, the radiative branch is most photon-like as $k_x \to \infty$, and the non-radiative branch is most photon-like as $k_x \to 0$. Finally, we note that in the non-radiative region, the surface electromagnetic waves decay exponentially with distance from the boundary of the two phases--they are evanescent waves.

The previous considerations applied only to a "smooth surface," the two-dimensional analog to the infinite, perfect crystal. However, we are interested in the coupling of light to surface plasmons in the low frequency region ($\omega < \omega_p$). There are two ways to do this:

1) Coupling of light to non-radiative surface plasmons using surface roughness (Grating coupling).

Imagine that a surface is quite smooth, except for a single step function at coordinate $x = \underline{a}$ such that $f(x) = 0$, $a \leq x \leq \infty$ but $f(x) = 1$, $0 \leq x < a$. The Fourier transform of this function is $\sqrt{\frac{2}{\pi}} \frac{\sin ak}{k}$. Similarly, the Fourier transform of a regular array of step functions, such as a diffraction grating, is described by a superposition of sine functions, characterized by a particular $\underline{k}$ vector, $\underline{k}_r = 2\pi d^{-1}$, where d = the grating constant. Finally, a rough surface can be viewed as a superposition of diffraction gratings. Thus, if a surface wave propagates along a rough surface, it has momentum $\hbar(\underline{k}_x + \underline{k}_r)$. Provided $\underline{k}_r$ is large enough, the resultant effective phase velocity $\omega/\underline{k}$ may then exceed c/n_d, and thus change a non-radiative surface wave into one that is

radiative. Equivalently, the effect of a grating may be viewed as providing additional momentum to the photons such that their phase velocity $\omega/(k_x + k_r)$ is reduced and becomes equal to that of the plasmons. The implications of this effect have been thoroughly discussed by Raether.[11] Experimental verification of grating coupling has been found by many workers.[13-16]

2) Excitation by evanescent waves (Prism coupling)

If the two-phase system we have been discussing is in contact with a transparent prism of refractive index n_p, so as to form the geometry illustrated in Fig. 3, and if light of frequency ω is incident upon the prism base at angle $\psi > \psi_c = \sin^{-1} (n_d/n_p)$, then that light will be totally reflected. Although no light is transmitted by the dielectric phase, there will be a surface wave which propagates along the prism-dielectric interface and which decays exponentially with the distance from the interface. The wave vector of this evanescent wave is

$$k_x = n_p(\omega/c) \sin \psi \qquad (14)$$

The changed dispersion curves are illustrated in Fig. 4. Over the range $n_p(\omega/c) < k_x < n_d(\omega/c)$ the lower branch has become radiative.

The three-phase system of prism + dielectric + metal is more complicated than the two-phase one used as a model, because there are more boundary conditions to be taken into account. At the dielectric-metal interface there are now evanescent waves in both the dielectric and the metal. The effect of the prism is then to couple both sets of waves in the dielectric phase, with

the result that photons are converted into surface plasmons over the range $n_p(\omega/c) < \underset{\sim}{k}_x < n_d(\omega/c)$. The attenuated total reflectance (ATR) can then be sampled by either an angular or frequency scan. In the latter case, for example, there will be a minimum in the reflectance when ω and $\underset{\sim}{k}_x$ satisfy the dispersion relation in the range stated above. Examples of this effect have been reviewed by Otto, who first correctly identified the effect.[17]

In Section VII we shall discuss possible mechanisms for the coupling of molecular excitations with those of the surfaces on which the molecules may be adsorbed. We close this section with the observation that the coupling of molecular excitations to surface plasmons closely resembles their coupling with light, since each interaction is dominated by the electric dipole operator. We can therefore look for the manifestation of this coupling in changed fluorescence widths, intensities or lifetimes, and in the intensity of Raman scattering by molecules on or near metal surfaces.[18,19] Similarly, we can expect that the same ways which can be used to couple light to surface plasmons (grating and prism coupling) will be of value in coupling molecular excitations to these surface excitation waves. In summary, we have come to appreciate that in the study of spectroscopic processes on metal surfaces, the surface itself is not passive, but may participate actively.

III. OPTIMIZATION OF EXPERIMENTAL GEOMETRY: INCIDENCE AND

     SCATTERING ANGLES, POLARIZATION AND ANALYSIS DIRECTIONS

The problem of calculating the relative intensity of light reflected at a boundary defined by two media having different optical constants as a function of the angle and polarization of the incident light is an old one.[20] By requiring continuity of the tangential components of both $\underset{\sim}{E}$ and $\underset{\sim}{H}$ at each boundary, Maxwell's equations can be solved for the ratios of the amplitudes of the reflected electric vectors, known as the Fresnel reflection coefficients. For non-normal incidence the exact expressions are cumbersome, and approximations must be used.[21] A numerical solution for particular selections of optical constants, appropriate to the infrared region, has been given by Greenler.[5] Using another set of optical constants appropriate to $\lambda = 488$ nm, Greenler and Slager extended these results to that wavelength.[4] Beginning in 1971 and continuing through 1976, McIntyre and co-workers published a series of papers in which, by the use of linear approximation theory, quite general forms of the <u>differential</u> reflectivity for different polarizations, as a function of angle were found.[6,22] In this theory, simplification of the Fresnel coefficients is achieved by the expansion of the exponential $e^{-2i\beta}$, where $\beta = \dfrac{2\pi \hat{n}_2 d \cos \varphi_2}{\lambda}$ is the phase change suffered by the light in a single traversal of a dielectric thin film (phase 2), and only terms that are linear in β are retained.[23] The approximation turns out to be quite

accurate when the film thickness $d << \lambda$, the wavelength of the incident light. The resulting expressions

$$\frac{\Delta R_\perp}{R_\perp} = \frac{8\pi d n_1 \cos \phi_1}{\lambda} \ \text{Im} \left(\frac{\hat{\epsilon}_2 - \hat{\epsilon}_3}{\epsilon_1 - \hat{\epsilon}_3} \right) \tag{15}$$

and

$$\frac{\Delta R_{||}}{R_{||}} = \frac{8\pi d n_1 \cos \phi_1}{\lambda} \text{Im} \left(\frac{\hat{\epsilon}_2 - \hat{\epsilon}_3}{\epsilon_1 - \hat{\epsilon}_3} \right) \left[\frac{1 - (\epsilon_1/\hat{\epsilon}_2 \hat{\epsilon}_3)(\hat{\epsilon}_2 + \hat{\epsilon}_3) \sin^2 \phi_1}{1 - (1/\hat{\epsilon}_3)(\epsilon_1 + \hat{\epsilon}_3) \sin^2 \phi_1} \right] \tag{16}$$

where ΔR_i = the <u>increase</u> in the reflectivity due to the presence of phase 2. The complex dielectric constant is related to the refractive index n and the extinction coefficient k by

$$\hat{\epsilon}_j = \epsilon'_j - i\epsilon''_j \tag{17}$$

$$\epsilon'_j = (n_j^2 - k_j^2)/\mu_j \tag{18}$$

and

$$\epsilon''_j = 2n_j k_j/\mu_j \tag{19}$$

Eqs. (17) - (19) are simplified in the visible and infrared regions since the magnetic permeabilities $\mu_j \cong 1$ there. Expressions for the reflectivities accurate to second order have been derived by Dignam et al.[24] The results are essentially the same as Eqs. (15) and (16).

Typical optical constants for a three-phase system consisting of (1) an ambient phase (vacuum or air or water), (2) a thin dielectric phase, and (3) a metal are given for the visible and

infrared regions in Table I. With these constants $\Delta R_\perp / R_\perp = 0$ in the infrared, for any angle. Greenler explained this result in terms of the relative amplitudes of the incident and reflected electric vectors of the radiation. Because an electric vector perpendicular to the plane of incidence must have a node at the surface of a highly reflecting surface, the coupling of the electromagnetic wave to the dielectric phase must then be very small. This observation was anticipated by Berreman, who recognized that because a metal is a conductor, the electrical field parallel to its surface must vanish at and near that surface.[25]

Greenler has also published a calculated *differential* reflectivity <u>vs</u>. angle of incidence curve for this same wavelength ($\lambda = 5.0 \ \mu m$),[5] but the function plotted is not quite the same as that calculated by McIntyre.[22] McIntyre defined $\Delta R/R$ as

$$\frac{\Delta R}{R} = \frac{R(d) - R(0)}{R(0)} \tag{20}$$

where $R(0) = R_{13}$ and $R(d) = R_{123}$, while Greenler plotted the function $A = (R^\circ - R)/R^\circ$, where R° is the reflectance of a three-phase system in which $k_2 = 0$. Since R_{13} does not depend on n_2, $\Delta R/R$ and A are not the same.

Ibach has shown that Eq. (16) can be further approximated by

$$\frac{\Delta R_{||}}{R_{||}} = \frac{8\pi d n_1 \ \sin^2 \phi_1}{\lambda \ \cos \phi_1} \ \mathrm{Im} \left(- \frac{1}{\epsilon_2} \right) \tag{21}$$

TABLE I

Optical Constants of a Typical Three-phase System
in the Visible and Infrared Regions

	$\lambda = 500$ nm	$\lambda = 5.0$ μm
n_1	1.333	1.000
n_2	3.0	1.3
k_2	1.5	0.1
n_3	2.0	3.0
k_3	4.0	30.0
d/λ	1.0×10^{-3}	1.0×10^{-4}

provided $\hat{\varepsilon}_3 \gg \hat{\varepsilon}_2 \gg \varepsilon_1 \approx 1.$[26] A similar expression was also given by Berreman.[24] This trigonometric dependence is monotone increasing throughout the range $0 \leq \mathcal{Q}_1 < \pi/2$, but the approximation is only valid if $\cos^2 \mathcal{Q}_1 > |\hat{\varepsilon}_3|^{-1}$. In this approximation, then, $\Delta R_{||}/R_{||}$ has an upper limit at the critical angle $\mathcal{Q}_c = \cos^{-1} [(\varepsilon_3')^2 + (\varepsilon_3'')^2]^{-\frac{1}{4}}$.

Because $-\Delta R = A_2 + \Delta A_3$, where A_2 is the surface-layer absorbance and ΔA_3 is the absorbance change in the metal due to the presence of the surface layer, and because $A_{||2} = A_{||2x} + A_{||2z}$ and $\Delta A_3 = \Delta A_{||3x} + \Delta A_{||3z}$ where the subscripts x and z refer to tangential and normal components of the absorbance (or absorbance change) respectively, it is possible to use linear approximation theory to dissect $\Delta R/R$ and thus discern the main contributors to its variation with incidence angle, especially in the vicinity of the critical angle. The result of this more careful analysis is that in the infrared, almost all of the variation in $\Delta R_{||}/R_{||}$ with $\mathcal{Q}_1$ is due to that of $A_{||2z}$, which goes through a real maximum (not just an upper limit) at $\mathcal{Q}_c$. Interestingly, $\Delta A_{||3}$ goes through a minimum at or near $\mathcal{Q}_c$. However, the dependence of $\Delta R_{||}/R_{||}$ on $\mathcal{Q}_1$ in the infrared mimics that of $A_{||2z}$, since $\Delta A_{||3}(\mathcal{Q}_1)$ is much the same for non-absorbing ($k_2 = 0$) and for absorbing surface films. For this reason, an absorption spectrum recorded at $\mathcal{Q}_c$ effectively has a flat background or "baseline."

In the visible region of the spectrum, however, while $A_{||2}$ again goes through a maximum (at an angle somewhat smaller than $\mathcal{Q}_c$

in the infrared), the maximum is not nearly as sharp as it is in
the infrared. Furthermore, while $\Delta A_{||3}$ again goes through a mini-
mum, it is different from $\Delta A_{||3}$ with a non-absorbing surface film.
Also, their minima are at different angles--and different from the
angle at which $A_{||2}$ is a maximum. The effect of all these
differences is that the angular variation of $\Delta R_{||}/R_{||}$ does not
resemble that of $A_{||2}$ at all. Instead, $\Delta R_{||}/R_{||}$ first goes
through a minimum at $\phi_1 = 60°$ and subsequently a small maximum
at $\phi_1 = 80°$. In fact, the percentage change $\Delta R_{||}/R_{||}$ is less
than 2.5% over the entire range $0 \leq \phi_1 \leq \pi/2$, so the angle of
incidence is hardly critical at all. (Even in the far infrared,
Berreman obtained excellent results with incidence angles in the
range 26 - 34°, far from ϕ_c.) Furthermore, in the visible
region, at $\phi_1 = 0°$

$$\frac{\Delta R_\perp}{R_\perp} = \frac{\Delta R_{||}}{R_{||}} \tag{22}$$

and, while these ratios have different dependences on $\phi_1 \neq 0$, their
absolute values do not vary much over the entire angular range.
The reason for this is that, largely because ε_3'' is so much smaller
in the visible region, $E_\perp$ does not vanish at the surface of a
metal. Hence, with visible excitation, perpendicular polariza-
tion becomes of practical utility. As we shall see in Sec. V,
this is of considerable importance in obtaining depolarization
ratios which are diagnostic for specific molecular orientations.

IV. SELECTION RULES FOR INFRARED AND RAMAN PROCESSES ON METAL SURFACES

There have been several suggestions that selection rules exist in infrared reflection-absorption spectroscopy (IRS) for molecules adsorbed on metal surfaces. Under the circumstances of high angles of incidence and parallel polarization, as required by the values of $\Delta R_\perp/R_\perp$ and $\Delta R_{||}/R_{||}$ in the infrared (See Sec. III), transitions for which the change in dipole moment is polarized perpendicular to the metal surface are effectively selected. The first experimental demonstration of this selection rule was by Berreman,[25] who studied evaporated films of LiF, in transmission on collodion, and in reflection on silvered glass. In the former case, the TO at 307 cm^{-1} is strongly absorbing but in the latter case the LO at $\sim$675 cm^{-1} dominates the spectrum.[27]

More recently, Pearce and Sheppard noted that a selection rule for IRS was not only demonstrated by the data of Francis and Ellison, who studied carboxylated ions adsorbed on metal surfaces,[28] but it is also substantiated in the spectra of ethylene adsorbed on a number of supported metal catalysts.[29] Next, Ibach observed that the same selection rule should apply in electron energy loss spectroscopy (ELS), since the scattering electron creates a field which also has no component parallel to the metal surface. Note too that for specularly reflected electrons the momentum loss due to inelastic collisions with the surface is normal to the surface.[26] Studies of acetylene and ethylene

adsorbed on Pt(111) by Ibach, Hopster and Sexton using ELS have demonstrated this selection rule.[30]

Pearce and Sheppard have described the metal surface selection rule for IRS in terms of the image charges and currents induced in a metal by a vibrating molecule which is adsorbed on its surface, the basis of which is the high polarizability of a metal.[31] A simple construction based upon the method of images then shows that a dipole parallel to the metal surface has an image dipole in the opposite direction, while the image of a dipole perpendicular to the surface is in the same direction as that of its source. In this model, the system which interacts with an external electromagnetic field is not the original charge distribution we call a molecule, but it is the system: molecule-plus-image. As a result, if the normal to the surface is denoted Z, only Z-polarized (out-of-plane) vibrations can be active; X- or Y-polarized (in-plane) vibrations must be spectroscopically inactive, in absorption.

We now inquire into the extension of this selection rule to Raman spectroscopy of metal surfaces. Pearce and Sheppard represented a vibrating dipole in its simplest form, as a pair of charges of opposite sign, with the internal coordinate of the vibration defined in the usual way.[32] The process of finding the image of each dipole is equivalent to the addition of a new symmetry

operation which characterizes the system of adsorbed molecule +
metal. This new operation consists of <u>simultaneous</u> reflection
in the plane of the metal surface, operating on the internal
coordinate, together with charge conjugation. Under this com-
bined operation, which we call $\underline{R}$, dipoles parallel to $\underline{Z}$ are left
invariant in magnitude and direction, but dipoles in the plane
perpendicular to $\underline{Z}$ are changed into their negatives. The system,
molecule + image, has a net dipole moment only for dipoles parallel
to $\underline{Z}$.

In group-theoretical terms this means that we must seek the
activity representations of the direct product group $\underline{M} = \underline{G} \otimes \{\underline{E} + \underline{R}\}$,
where $\underline{G}$ is the point group of the molecule and $\underline{R}$ is the combined
operation, $\sigma_h \underline{C}$ ($\underline{C}$ = charge conjugation). Since $\underline{R}^2 = \underline{E}$ and $\underline{R}$
commutes with all members of $\underline{G}$, we can classify the representa-
tions of $\underline{G}$ in terms of those of $\{\underline{E} + \underline{R}\}$ with which each correlates.
The requirement that the significant dipole moment is that of the
system, molecule + image, means that only the "in-phase" combina-
tions of the motions of the source molecule with those of its
image are spectroscopically active. Thus, the activity represen-
tations of $\{\underline{E} + \underline{R}\}$ are all totally symmetric. In other words,
the activity representations of $\underline{G}$ are just those which are
invariant under $\underline{R}$.

This was implicit in the selection rules for IRS derived
by Pearce and Sheppard,[29] in that the transformation properties
of the cartesian components of a vector under the operation $\underline{R}$ were

found.   These were

$$\underline{R} \begin{pmatrix} X \\ Y \\ Z \end{pmatrix} = \begin{pmatrix} -X \\ -Y \\ Z \end{pmatrix} \tag{23}$$

or

$$\underline{R} = \begin{pmatrix} -1 & 0 & 0 \\ 0 & -1 & 0 \\ 0 & 0 & 1 \end{pmatrix} \tag{24}$$

Thus $\chi(\underline{R}) = -1$.   The group $\{\underline{E} + \underline{R}\}$ is seen to be isomorphous with $\underline{C}_2$. $\Gamma_{\underline{Z}} = \underline{A}$, $\Gamma_{\underline{X}} = \Gamma_{\underline{Y}} = \underline{B}$ but, as we have seen, $\underline{A}$ is the only activity representation.

The extension to obtain selection rules for Raman spectra on metal surfaces is carried out by examining the transformation properties of the components of the polarizability tensor under the operation $\underline{R}$.   Because of the transformation properties of the cartesian components of a vector as given above, and because the polarizability tensor is a symmetric tensor of the second rank, $\Gamma_{\underline{Z}^2} = \Gamma_{\underline{X}^2} = \Gamma_{\underline{Y}^2} = \Gamma_{\underline{XY}} = \underline{A}$, but $\Gamma_{\underline{XZ}} = \Gamma_{\underline{YZ}} = B$.   Again, $\underline{A}$ is the only activity representation.   In effect, the $\underline{XZ}$ and $\underline{YZ}$ components of the derived polarizability tensor for the system molecule + image vanish, while all other components do not.

These rules can be the basis of a valuable technique for the determination of molecular orientation on metal surfaces. For example, if a $\underline{C}_{2v}$ molecule is adsorbed on a metal surface, the several tensor components which may appear in the Raman spectrum depend on molecular orientation in the manner shown in Table II.

TABLE II

Raman-active Polarizability Tensor Components for an
Adsorbed Molecule with C_{2v} Symmetry

$\underline{z}||\underline{Z}$ (end-on)	$\underline{x}||\underline{Z}$ (flat)	$\underline{y}||\underline{Z}$ (on edge)
$A_1\,(\underline{x}^2,\underline{y}^2,\underline{z}^2)$	$A_1\,(\underline{x}^2,\underline{y}^2,\underline{z}^2)$	$A_1\,(\underline{x}^2,\underline{y}^2,\underline{z}^2)$
$A_2\,(\underline{xy})$	$B_2\,(\underline{yz})$	$B_1\,(\underline{xz})$

In addition to this kind of prediction, it is possible to design Raman scattering experiments such that the directions of the incident and scattered rays and their polarization directions are chosen so as to enable the determination of particular polarizability tensor elements from the observed Raman intensities. This procedure is quite analogous to a well-established one used in the study of the Raman spectra of solids,[33] and augments that used in the study of fluids in which a depolarization ratio is calculated.[34] Since there has been some confusion in the application of this calculation to surfaces, and because the results supplement the predictions of Table II, we shall present this procedure in the next section.

The direct product group $\underline{M} = \underline{G} \otimes \{\underline{E} + \underline{R}\}$ is an example of a Type II Shubnikov point group, sometimes called a grey point group.[35] In Shubnikov groups, $\underline{R}$ is an extra coordinate, one which has only two possible values, such as black or white, or positive or negative. In the case of grey groups, the extra coordinate assumes both of its values simultaneously; hence, grey. A little reflection will show that the combined operation, $\underline{R} = \sigma_h \underline{C}$, has this property.

Furthermore, if an adsorbed monolayer is truly oriented, it should be viewed as a two-dimensional, semi-infinite crystal. Then the vibrations of the molecules in such a layer should be analyzed, not in terms of the irreducible representations of the molecular point group, but in terms of those of one or another of the 17 possible two-dimensional space groups.[36] All so-called lattice reconstructions are Bravais lattices or superlattices of these space groups. In view of the special role played by the operator $\underline{R} = \sigma_h\underline{C}$ in determinining the selection rules of molecules adsorbed on metal surfaces, the two-dimensional space groups of interest are all grey.[37] That is,

$$\underline{M} = \underline{G} + R\underline{G} \tag{25}$$

where R is a space group operation, $\{\underline{R}|\underline{v}\}$.

The 17 two-dimensional grey space groups have all been tabulated by Belov.[38] For convenience, the tabulation is repeated in Table III. As noted by Belov, the "three-dimensional" unit cells of the 17 grey groups have twice the "height" of the 17 ordinary two-dimensional space groups from which they are derived. Each grey group will therefore have twice as many phonon branches as did its symmorphic parent. Half of these will be symmetric combinations of the vibrational modes of the source molecules and their images, and the other half will be antisymmetric combinations. As we have seen, only the symmetric combinations may include those which are spectroscopically active.

TABLE III

Ordinary and Grey Space Groups

Ordinary		Grey	
C_1^1	(p1)	C_s^1	(pm)
C_2^1	(p2)	C_{2h}^1	(p2/m)
C_s^1	(pm)	C_{2v}^1	(pmm2)
C_s^2	(pg)	C_{2v}^7	(pgm2$_1$)
C_s^3	(cm)	C_{2v}^{11}	(cmm2)
C_{2v}^1	(pmm)	D_{2h}^1	(pmmm)
C_{2v}^4	(pmg)	D_{2h}^5	(pmma)
C_{2v}^8	(pgg)	D_{2h}^9	(pbam)
C_{2v}^{11}	(cmm)	D_{2h}^{19}	(cmmm)
C_4^1	(p4)	C_{4h}^1	(p4/m)
C_{4v}^1	(p4m)	D_{4h}^1	(p4/mmm)
C_{4v}^2	(p4g)	D_{4h}^5	(p4/mbm)
C_3^1	(p3)	C_{3h}^1	(p$\bar{6}$)
C_{3v}^1	(p3m1)	D_{3h}^1	(p$\bar{6}$m2)
C_{3v}^2	(p31m)	D_{3h}^3	(p$\bar{6}$2m)
C_6^1	(p6)	C_{6h}^1	(p6/m)
C_{6v}^1	(p6m)	D_{6h}^1	(p6/mmm)

As an example, in Table IV we illustrate these matters using the point group $\underset{\sim}{G} = \underline{C}_{2\underline{v}}$, for which the direct product $\underset{\sim}{M} = \underline{C}_{2\underline{v}} \otimes \{\underline{E} + \underline{R}\} = \underline{D}_{2\underline{h}}$. The activity representations are all in the upper half of the table. In addition, a symmetric combination is shown graphically in Fig. 5.

As in three dimensions, correlation of the molecular point group with the appropriate space group is facilitated by knowledge of its sites.[39] The sites of the 17 two-dimensional space groups are given in Table V. In any case, space group theory should be used in order to carry out a correct symmetry analysis of multiphonon transitions.[40] This will be particularly true with CARS.[41] Otherwise the point group isomorphous with the space group at $\underset{\sim}{k} = 0$ suffices. While correlation of the motions at $\underset{\sim}{k} \neq 0$ is usually a sufficient guide to correct selection rules, it may fail at certain points in the two-dimensional Brillouin zone because of additional degeneracies due to time-reversal symmetry.[42] A list of all such degeneracies has been given by Cracknell.[37]

We conclude this section with three conjectures which have to do with limits and extensions of these selection rules:

1. In addition to metals, the surface selection rules should apply to insulators at frequencies where they have metallic reflectance.

2. The surface selection rules should lose their validity as $\omega > \omega_{sp}$.

TABLE IV

Correlations Between the Groups $\{\underline{E} + \underline{R}\}$, $\underset{\sim}{G} = \underline{C}_{2\underline{v}}$ and $\underset{\sim}{M} = \underset{\sim}{G} \otimes \{\underline{E} + \underline{R}\}$

$\{\underline{E} + \underline{R}\}$	$\underset{\sim}{G} = \underline{C}_{2\underline{v}}$	$\underset{\sim}{M} = \underset{\sim}{G} \otimes \{\underline{E} + \underline{R}\} = \underline{D}_{2\underline{h}}$

$\underline{A}$ $(\underline{Z}; \underline{X}^2, \underline{Y}^2, \underline{Z}^2, \underline{XY})$

$\underline{A}_1$ $(\underline{Z}; \underline{X}^2, \underline{Y}^2, \underline{Z}^2)$

$\underline{A}_g$ $(\underline{X}^2, \underline{Y}^2, \underline{Z}^2)$

$\underline{B}_{1u}$ $(\underline{Z})$

$\underline{A}_2$ $(\underline{XY})$

$\underline{B}_{1g}$ $(\underline{XY})$

$\underline{A}_u$ $---$

$\underline{B}$ $(\underline{X}, \underline{Y}; \underline{XZ}, \underline{YZ})$

$\underline{B}_1$ $(\underline{X}; \underline{XZ})$

$\underline{B}_{2g}$ $(\underline{XZ})$

$\underline{B}_{3u}$ $(\underline{X})$

$\underline{B}_2$ $(\underline{Y}; \underline{YZ})$

$\underline{B}_{3g}$ $(\underline{YZ})$

$\underline{B}_{2u}$ $(\underline{Y})$
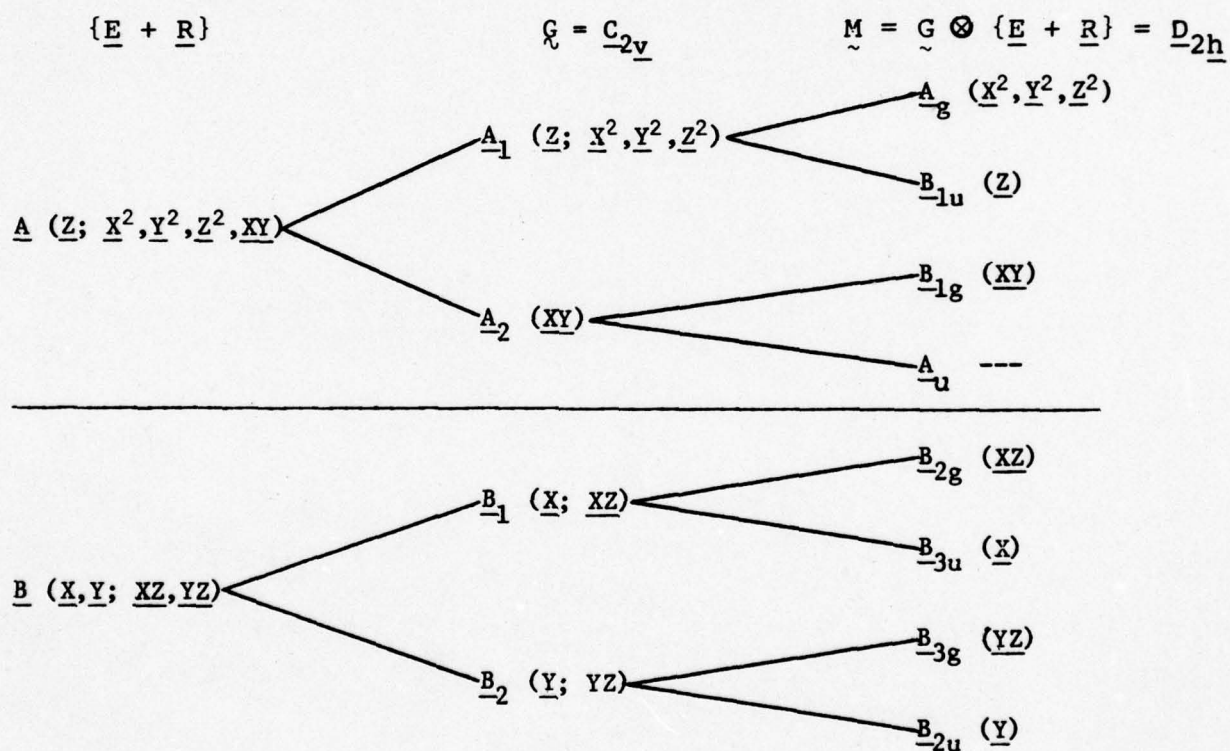
TABLE V

Sites of the Seventeen Two-Dimensional Space Groups

System	International Symbol	Schönflies Symbol	C_{6v}	C_6	C_{4v}	C_4	C_{3v}	C_3	C_{2v}	C_2	C_s	C_1
Oblique	p1	C_1^1										a
	p2	C_2^1							a-d			e
Rectangular	pm	C_s^1									a,b	c
	pg	C_s^2										a
	cm	C_s^3									a	b
	pmm	C_{2v}^1							a-d		e-h	i
	pmg	C_{2v}^4							a,b		c	d
	pgg	C_{2v}^8							a,b			c
	cmm	C_{2v}^{11}							a,b	c	d,e	f
Square	p4	C_4^1				a,b				c		d
	p4m	C_{4v}^1			a,b				c	d-f		g
	p4g	C_{4v}^2				a			b		c	d
Hexagonal	p3	C_3^1						a-c				d
	p3m1	C_{3v}^1					a-c				d	e
	p31m	C_{3v}^2					a	b			c	d
	p6	C_6^1		a				b		c		d
	p6m	C_{6v}^1	a				b		c		d,e	f

3.   Because the electric field due to the surface electro-
magnetic waves decays according to e^{-kz} in the vicinity of the
surface, the effect of transparent dielectrics, in between the
metal surface and the adsorbate layer should be negligible,
provided $\varepsilon_d \sim 1$. Thus, if the metal substrate has a thin oxide
layer, the metal surface selection rules should still be valid.
For the same reason, it may be possible to obtain similar spectra
by depositing a thin metal layer on one side of a dielectric sub-
strate--the metal serving to "short out" the transverse modes.

V.   DEPOLARIZATION OF RAMAN SCATTERING FROM METAL SURFACES: THE
      DETERMINATION OF MOLECULAR ORIENTATION

In carrying out a right-angled Raman scattering experiment
on a metal surface using oblique incidence and TM polarization,
two scattering geometries are possible, both illustrated in
Fig. 6. The metal surface is taken as the XY plane and the i(pa)s
notation is used.[43] We assume that in each possible experiment
all molecules are similarly aligned with respect to the surface
axes. For purposes of illustration we discuss a molecule with
point symmetry C_{2v}. Molecular axes are designated by x, y, z
and surface axes by X, Y, Z.

The two scattering geometries are distinguished as follows.
In the first we shall discuss, the exciting radiation is incident
on the surface XY 45° off the normal, and the scattering is viewed
on the surface edge (i.e., s||X). In the second scattering

geometry illustrated in Fig. 6, the light is incident in the same way, but the scattered light is viewed near the direction of specular reflection.

As in the case of crystals, it is sometimes useful to choose the plane of polarization such that it is not parallel to the laboratory axes. The polarizability tensor is then subjected to an orthogonal transformation corresponding to this rotation. We first illustrate this with the geometry $\underline{i}(\underline{pa})\underline{s} = \underline{Y}\text{-}\underline{Z}\left(\underline{Y} + \underline{Z}, \begin{Bmatrix} \underline{Y} - \underline{Z} \\ \underline{Y} + \underline{Z} \end{Bmatrix}\right)\underline{X}$, in which the orthogonal transformation matrix is

$$R = \begin{pmatrix} 1 & 0 & 0 \\ 0 & \frac{1}{\sqrt{2}} & \frac{1}{\sqrt{2}} \\ 0 & -\frac{1}{\sqrt{2}} & \frac{1}{\sqrt{2}} \end{pmatrix}$$

We consider two molecular orientations:

    i. $\underline{z}||\underline{Z}, \ \underline{y}||\underline{X}, \ \underline{x}||\underline{Y}$ (end-on)

    ii. $\underline{x}||\underline{Z}, \ \underline{y}||\underline{X}, \ \underline{z}||\underline{Y}$ (flat)

<u>Case i</u>. The molecule is "attached" end-on to the surface.

The molecular polarizability tensors have the form

$$\underset{\sim}{\alpha}\underline{a}_1 = \begin{pmatrix} \underline{a} & & \\ & \underline{b} & \\ & & \underline{c} \end{pmatrix} \quad ; \quad \underset{\sim}{\alpha}\underline{b}_1 = \begin{pmatrix} & & \underline{e} \\ & & \\ \underline{e} & & \end{pmatrix}$$

$$\underset{\sim}{\alpha}\underline{a}_2 = \begin{pmatrix} & \underline{d} & \\ \underline{d} & & \\ & & \end{pmatrix} \quad ; \quad \underset{\sim}{\alpha}\underline{b}_2 = \begin{pmatrix} & & \\ & & \underline{f} \\ & \underline{f} & \end{pmatrix}$$

In the "surface frame" (laboratory axes), these become

$$\alpha_{\underset{\sim}{A}_1} = \begin{pmatrix} \underline{b} & & \\ & \underline{a} & \\ & & \underline{c} \end{pmatrix} \quad ; \quad \alpha_{\underset{\sim}{B}_1} = \begin{pmatrix} & & \underline{f} \\ & & \\ \underline{f} & & \end{pmatrix}$$

$$\alpha_{\underset{\sim}{A}_2} = \begin{pmatrix} & \underline{d} & \\ \underline{d} & & \\ & & \end{pmatrix} \quad ; \quad \alpha_{\underset{\sim}{B}_2} = \begin{pmatrix} & & \\ & & \underline{e} \\ & \underline{e} & \end{pmatrix}$$

The result of the orthogonal transformation, so as to conform with the stated polarization and analysis directions, is:

$$\alpha_{\underset{\sim}{A}_1} = \begin{pmatrix} \underline{b} & 0 & 0 \\ 0 & \dfrac{\underline{a}+\underline{c}}{2} & \dfrac{\underline{c}-\underline{a}}{2} \\ 0 & \dfrac{\underline{c}-\underline{a}}{2} & \dfrac{\underline{a}+\underline{c}}{2} \end{pmatrix} \quad ; \quad \alpha_{\underset{\sim}{B}_1} = \underline{f}/\sqrt{2}\begin{pmatrix} 0 & 1 & 1 \\ 1 & 0 & 0 \\ 1 & 0 & 0 \end{pmatrix}$$

$$\alpha_{\underset{\sim}{A}_2} = \underline{d}/\sqrt{2}\begin{pmatrix} 0 & 1 & -1 \\ 1 & 0 & 0 \\ -1 & 0 & 0 \end{pmatrix} \quad ; \quad \alpha_{\underset{\sim}{B}_2} = \underline{e}\begin{pmatrix} 0 & 0 & 0 \\ 0 & 1 & 0 \\ 0 & 0 & -1 \end{pmatrix}$$

We recall from Sec. IV that in this case $\underline{A}_1$ and $\underline{A}_2$ are the only activity representations. For the two polarizations, the relative intensities of the $\underline{A}_1$ modes are

$$I_{||} = I(\underline{Y} + \underline{Z}, \ \underline{Y} + \underline{Z}) = (\underline{a} + \underline{c})^2/4 \tag{26}$$

$$I_{\perp} = I(\underline{Y} + \underline{Z}, \ \underline{Y} - \underline{Z}) = (\underline{a} - \underline{c})^2/4 \tag{27}$$

so that the depolarization ratio is

$$\rho_{\ell} = I_{\perp}/I_{||} = \left(\frac{\underline{a} - \underline{c}}{\underline{a} + \underline{c}}\right)^2 \tag{28}$$

Case ii

A similar analysis can be carried out for the case where a C_{2v} molecule lies flat on the surface ($\underline{x}||\underline{Z}$, $\underline{y}||\underline{X}$, $\underline{z}||\underline{Y}$). The several polarizability tensors are:

Molecule   Surface

$$\begin{pmatrix} \underline{a} & & \\ & \underline{b} & \\ & & \underline{c} \end{pmatrix}_{\underline{a}_1} \rightarrow \begin{pmatrix} \underline{b} & & \\ & \underline{c} & \\ & & \underline{a} \end{pmatrix}_{\underline{A}_1} \overset{\text{R}}{\rightarrow} \begin{pmatrix} \underline{b} & & \\ & \frac{\underline{a}+\underline{c}}{2} & \frac{\underline{a}-\underline{c}}{2} \\ & \frac{\underline{a}-\underline{c}}{2} & \frac{\underline{a}+\underline{c}}{2} \end{pmatrix}$$

$$\begin{pmatrix} & \underline{d} & \\ \underline{d} & & \\ & & \end{pmatrix}_{\underline{a}_2} \rightarrow \begin{pmatrix} & \underline{d} & \\ & & \\ \underline{d} & & \end{pmatrix}_{\underline{B}_1} \overset{\text{R}}{\rightarrow} \frac{\underline{d}}{\sqrt{2}}\begin{pmatrix} 0 & 1 & 1 \\ 1 & 0 & 0 \\ 1 & 0 & 0 \end{pmatrix}$$

$$\begin{pmatrix} & & \underline{e} \\ & & \\ \underline{e} & & \end{pmatrix}_{\underline{b}_1} \rightarrow \begin{pmatrix} & & \\ & & \underline{e} \\ & \underline{e} & \end{pmatrix}_{\underline{B}_2} \overset{\text{R}}{\rightarrow} \underline{e}\begin{pmatrix} 0 & 1 & 0 \\ 0 & 1 & 0 \\ 0 & 0 & -1 \end{pmatrix}$$

$$\begin{pmatrix} & \underline{f} & \\ & & \underline{f} \\ \underline{f} & & \end{pmatrix}_{\underline{b}_2} \rightarrow \begin{pmatrix} & \underline{f} & \\ \underline{f} & & \\ & & \end{pmatrix}_{\underline{A}_2} \overset{\text{R}}{\rightarrow} \frac{\underline{f}}{\sqrt{2}}\begin{pmatrix} 0 & 1 & -1 \\ 1 & 0 & 0 \\ -1 & 0 & 0 \end{pmatrix}$$

Now the activity representations are $\underline{A}_1$ and $\underline{B}_2$. The relative intensities and depolarization of the $\underline{A}_1$ modes for two polarizations are the same as in Case $\underline{i}$ [Eqs. (26), (27) and (28)]. Therefore, in this scattering geometry (incident radiation viewed on the surface eged) the "end-on" and "flat" molecular orientation cannot be distinguished using polarization measurements. These

results, together with those for two other molecular orientations, are displayed in Table VI.

For the second scattering geometry illustrated in Fig. 6 (scattered light viewed close to the direction of specular reflection), the procedures are the same as those used with the first geometry. Although $I_{||}$ equals $(\underline{a} - \underline{c})^2/4$ for Cases $\underline{i}$ and $\underline{ii}$ and $(\underline{b} - \underline{c})^2/4$ for Cases $\underline{iii}$ and $\underline{iv}$, $I_{\perp}$ and therefore ρ_ℓ is zero in all four cases.[44] If depolarization ratios are desired for this geometry, illumination with unpolarized light should be used. Then, for example, in Case $\underline{iii}$, $\rho_n = 2\underline{a}^2[(\underline{b} + \underline{c})^2 + 2\underline{a}^2]^{-1}$. Since, in this geometry, more than one polarization of the incident light is used, the observed depolarization ratio should be corrected for the differential reflectivities of the light with each polarization (See Sec. III).

It is therefore possible to draw some conclusions from observed depolarization factors concerning the relative orientation of molecules on surfaces, but only in a limited way. If the components of the molecular polarizability tensors ($\underline{a}$ - $\underline{f}$) are known from, say, single crystal studies, the method would then be quite powerful. We reemphasize that we have assumed that, in any one "molecular orientation," all adsorbed molecules are similarly aligned. If they are not, then the Snyder's procedures for systems of partially oriented molecules should be used.[46]

TABLE VI

Scattering Geometry 1 (See Fig. 6)

Molecular Orientation	$I_\perp$	$I_{||}$	$\rho = I_\perp/I_{||}$
i[z$||$Z, y$||$X, x$||$Y]	$(\underline{a} - \underline{c})^2/4$	$(\underline{a} + \underline{c})^2/4$	$(\underline{a} - \underline{c})^2/(\underline{a} + \underline{c})^2$
ii[x$||$Z, y$||$X, z$||$Y]	$(\underline{a} - \underline{c})^2/4$	$(\underline{a} + \underline{c})^2/4$	$(\underline{a} - \underline{c})^2/(\underline{a} + \underline{c})^2$
iii[z$||$Z, x$||$X, y$||$Y]	$(\underline{b} - \underline{c})^2/4$	$(\underline{b} + \underline{c})^2/4$	$(\underline{b} - \underline{c})^2/(\underline{b} + \underline{c})^2$
iv[y$||$Z, x$||$X, z$||$Y]	$(\underline{b} - \underline{c})^2/4$	$(\underline{b} + \underline{c})^2/4$	$(\underline{b} - \underline{c})^2/(\underline{b} + \underline{c})^2$

VI. EXPERIMENTAL RAMAN AND OTHER SURFACE SPECTROSCOPIC INVESTI-
     GATIONS OF METAL SURFACES

In Section IV we have already mentioned the pioneering work
of Berreman and of Pearce and Shepperd, whose infrared spectro-
scopic investigations and interpretations first suggested the
presence of metal surface selection rules. In this section we
shall discuss other spectroscopic studies which have been made,
and in particular some recent Raman scattering studies, with
which the predictions made in the last two sections can be
tested. We begin, however, with a similar discussion of the
infrared results, as well as those of related techniques, such
as ELS.

A.   IRS and related spectroscopies

The fundamental observation, which forms the foundation of
the entire subject of metal surface selection rules, is that of
Berreman, who confirmed his expectation that, in the infrared
reflection-absorption spectrum of LiF films evaporated onto
silver, the spectrum with parallel polarization is dominated by
the LO mode of LiF.[25] Interestingly, the film thicknesses used
were 325-348 nm; hence, the sample was far from being a monolayer.
Nothwithstanding this thickness, we can conclude that the metal
surface selection rule governed the entire sample, since the TO
was apparently quite inactive.

Pearce and Sheppard began their interpretation of the spectrum of adsorbed ethylene with the assumption that the adsorbed species is a "molecule" of the type MCH_2CH_2M, with point symmetry $\underset{\sim}{C}_{2v}$, where M is a surface metal atom. For experimental reasons, they concentrated on the CH stretching modes in the 2700-3000 cm^{-1} region. Although four different stretching modes are obviously possible, only two bands were detected in this region with each of the metals studied (Pt, Pd, Ni and Ph), and one of these bands is certainly an overtone of a CH_2 scissors mode. In $\underset{\sim}{C}_{2v}$ symmetry, the four possible stretching modes are equally distributed among each of the irreducible representations of $\underset{\sim}{C}_{2v}$. The metal surface selection rule, however, permits only modes belonging to $\underset{\sim}{A}_1$ of $\underset{\sim}{C}_{2v}$, since it is the only irreducible representation that is an activity representation of $\underset{\sim}{G} = \underset{\sim}{C}_{2v}$ (See Table IV).

Ibach has also studied adsorbed C_2H_4, using ELS. As indicated in Sec. IV, the same selection rules should apply to ELS as in IRS.[47] On Pt(111) four resonances are observed, corresponding to 2920, 1411, 1000 and 419 cm^{-1}. On the basis of interpretations of ultraviolet photoelectric spectra, ethylene is thought to lie flat on the metal surface (as far as the carbon atoms are concerned), and to have point symmetry $\underset{\sim}{C}_{2v}$.[48] The metal surface selection rule would then permit observation of those modes of C_2H_4 in the gas phase, where it has point symmetry $\underset{\sim}{D}_{2h}$, which correlate with $\underset{\sim}{C}_{2v}$. These are

$\nu_1^{CH\ s\ str} = 3026\ cm^{-1}$, $\nu_2^{CC} = 1623\ cm^{-1}$, $\nu_3^{CH_2\ scis} = 1342\ cm^{-1}$ and $\nu_7^{CH_2\ wag} = 949\ cm^{-1}$. Only one of the ELS resonances (2920 cm^{-1}) can be compared with the observations of Pearce and Sheppard, who observed ν_1 on Pt at 2880 cm^{-1}. Ibach has assigned the ELS resonances at 1411 and 1000 cm^{-1} to ν_3 and ν_7, respectively, while the resonance at 419 cm^{-1} is ascribed to a Pt-C vibration. However, according to the symmetry analysis, this mode must still have a large component due to carbon-carbon stretching. It is of course to be expected that chemisorbed ethylene will have different vibrational frequencies from those of the free molecule, and that ν_1 will be changed least. As Ibach pointed out, the analog of ν_3 in CH_2Cl_2 lies at 1467 cm^{-1}. Why ν_7 is changed so little (it lies at 1268 cm^{-1} in CH_2Cl_2) has not been addressed.

Ibach has also studied acetylene adsorbed on Pt(111). Again the molecule is thought to lie flat on the metal surface. In this case, correlation of $\underline{D}_{2h}$ with $\underline{C}_{2v}$ predicts that three fundamentals should be active, ν_1^{CH}, ν_2^{CC} and one component of ν_5, observed in the gas phase at 3374, 1974 and 730 cm^{-1}, respectively. Three resonances are observed in ELS at 3025, 1428 and 766 cm^{-1}. In C_2D_2, the gas phase frequencies are 2701, 1762 and 537 cm^{-1}; the ELS resonances lie at 2259, 1275 and 581 cm^{-1}.

There is still another electron scattering technique with selection rules similar to those of IRS and ELS. This is the technique of inelastic electron tunneling spectroscopy (IETS), first proposed by Scalapino and Marcus[49] and demonstrated by Lambe and Jaklevic.[50] More recently, the technique has been developed by

Hansma.[51] Dipole selection rules should govern this effect, too.[49,50,52] As with IRS and ELS, provided the molecules are all oriented in the oxide-metal phase that is so necessary in this technique, only out-of-plane molecular vibration modes can be active. While there is some evidence for orientation in the case of a benzoic acid-doped alumina-lead tunneling junction,[52] a careful study of a similar junction doped with anthracene showed no evidence of orientation.[53] On the other hand, there is considerable evidence in this and other studies, that Raman-active modes become weakly allowed in IETS. It is to be noted that in this technique the dielectric phase is far from a monolayer.

The metal surface selection rules therefore seem to be reasonably well obeyed in IRS and ELS, less so in IETS, but possibly for good reason--the system and the scattering mechanism in this technique are both more complex.

B.   Raman scattering

Burstein and coworkers have studied Raman scattering from a variety of surfaces, beginning with studies of doped InSb crystals.[54] In this case, the appearance of the $k \cong 0$ LO in the $\underline{Y}'(\underline{X}'\underline{X}')\underline{Y}'$ geometry ($\underline{Y}' = [110]$, $\underline{X}' = [1\bar{1}1]$ was ascribed to a lowering of the crystal symmetry at the surface due to the presence of a surface electric field of the order of 10^5 volts/cm.[55] The high surface field is claimed to be the result of a depletion layer near the surface which is evidenced by the lack of dependence of the LO frequency on the carrier concentration.

In addition, there have been brief reports of enhanced Raman scattering by Rhodamine 6G dye adsorbed on Ag.[56] Chen et al. have also examined the expressions for the differential Raman scattering cross section of a thin layer on a metal surface, in both ordinary reflection and in the ATR configuration (See Sec. II), and find that at particular scattering angles the scattering efficiency should be sharply peaked.[57] In ordinary reflection the critical incidence and scattering angles are just those discussed in Sec. III; in ATR, the critical angle is that of the coupling prism. The calculated "enhancements" in the two cases are by factors of 3 and 10^3. In a "mixed" configuration, using a prism to couple the incident radiation to the surface but without coupling the scattered radiation with a prism, the calculated enhancement is approximately 10^2. In one of the brief reports cited above, measurements of Raman scattering by benzene on Ag in this configuration indicated an enhancement by a factor of 75.[57]

During the past year Cooney et al have reported Raman scattering by the diatomic molecules I_2 and CO adsorbed on Pt electrodes,[58,59] and by SCN^- on a Ag electrode.[60] The fact that the spectra of I_2 and CO are of comparable intensity may be significant, as their polarizability derivatives, calculated by the method of Long and Plane,[61] differ by a factor of $10^{\frac{1}{2}}$. Since the fundamental vibrations of both molecules are totally symmetric, their detection can give no information about molecular orientation.

The same is true with respect to the stretching vibrations of SCN$^-$, such as ν_1, which has also been observed.[60] However, it would be possible to determine the orientation of SCN$^-$ had its bending mode been detected, for it can only scatter if the molecular axis is parallel to the surface. Unfortunately, only the high frequency region of the spectrum ($\Delta\nu$ = 2000 - 2200 cm^{-1}) was reported.

McQuillan, Hendra and Fleischmann were the first to report the Raman spectrum of pyridine adsorbed on a roughened Ag electrode.[62] The signal-to-noise ratio in the unaveraged spectrum appears to be greater than those of the signal-averaged spectra of I$_2$, CO and SCN$^-$ cited above. This qualitatively supports the estimates made in two other reports that Raman bands due to adsorbed pyridine are 10^5 - 10^6 times stronger than those due to aqueous or liquid pyridine.[45,63] The following calculation indicates the basis of these estimates.

A sample of liquid pyridine scatters from a volume defined by the focal region of the collection optics used in a Raman experiment. The length and waist of that region are defined by the wavelength of the light and by the effective aperture of the collection optics.[64] The effective aperture is the ratio α of the diameter of the laser beam to the focal length of the collection lens. The scattering volume is approximately $V = 32 \lambda^3/\pi^2\alpha^4$. [For a lens with focal length of 15 cm, $V \cong$ 2 - 5 nl, depending on wavelength (458 - 633 nm).]

If the laser beam is incident upon a Ag electrode at an angle of incidence ℓ measured from the normal, the electrode forms a projected image of the waist of the focal region with an area that also depends on the wavelength and the effective aperture. The scattering area is approximately A = 4 $\lambda^2/\pi\alpha^2$ cos^2 ℓ. [For a lens with f = 15 cm and with ℓ = 2π/6, the area has a diameter of $\sim$60 - 80 μm.]

Using a silver electrode immersed in liquid pyridine, Raman lines can be simultaneously detected that correspond to the same fundamental mode of vibration [e.g., $\nu_9(a_1)$] in the two phases-- the liquid and the adsorbed layer. They have slightly different frequencies -- 991 cm^{-1} in the liquid and 1006 cm^{-1} on Ag. If there is no special enhancement of the intensity of either phase, the relative intensity of the two lines ought to be given by I_{liq}/I_{ads} = $\rho_\ell V/\rho_s A$, where ρ_ℓ and ρ_s are the number densities of the two phases. For the liquid $\rho_\ell \cong$ 7.5 x 10^{21} cm^{-3}. The adsorption isotherm of pyridine on Ag indicates that only mono-layers of the molecule are adsorbed on that surface.[65] Assuming a particular and common orientation of pyridine molecules, ρ_s = 9.0 x 10^{14} cm^{-2}, approximately the same as one per Ag atom (100 face).

Under these circumstances, the ratio I_{liq}/I_{ads} = (2.0 $\pm$ 0.3) x 10^4, the variation being due to the wavelength dependence of the focal region waist. However, using Ar 488.0 nm excitation, it has been found that the two lines (991 and 1006 cm^{-1}) have com-parable intensity. Hence, the intensity enhancement of the Raman

spectrum of adsorbed pyridine appears to be by a factor of approximately 10^4. In making this calculation we have assumed a surface roughness factor of 3.5. More extensive surface roughness could account for the intensity enhancement, of course, but the _effective_ surface number density would then have to be four orders of magnitude larger than one per Ag atom.

In their investigation of the Raman spectrum of pyridine adsorbed on a Ag electrode, Jeanmaire and Van Duyne found six strong lines, all of which correspond to totally symmetric fundamental modes (3056, 1594, 1215, 1035, 1006 and 623 cm^{-1}).[45] In addition, they reported 16 weak lines, most of which are overtones or combinations. Of the remaining fundamentals, 7 have been confirmed in this laboratory. Two of these correspond to b_1 modes (942 and 405 cm^{-1}) and all others (1572, 1439, 1148 and 652 cm^{-1}) correspond to b_2 modes. No frequencies corresponding to a_2 modes have been observed. According to Table II, therefore, "end-on" adsorption is not favored. This conclusion is quite independent of the scattering geometry used. The spectrum of pyridine adsorbed on Ag thus qualitatively supports the idea of oriented adsorption. A quantitative determination of the orientation awaits measurements of the depolarization ratios ρ_ℓ and ρ_n, using several scattering geometries.

As noted above, the Raman spectrum of pyridine adsorbed on Ag is apparently unusually intense. In addition, that intensity depends on the excitation frequency, and in an unusual way. We shall discuss the basis of both of these observations in the next section, but first, three important questions remain:

1)   What is the precise chemical nature of the surface on which the pyridine is adsorbed (i.e., is it pure Ag)?

2)   What is the precise physical nature of the surface on which the pyridine is adsorbed (i.e., what is the surface roughness)?

3)   If the surface is chemically impure or rougher than we have supposed, does either make a difference with respect to our conclusions about selection rules and relative intensities?

The first two questions have been the subjects of an intensive study in our laboratory in which we have used secondary ion mass spectroscopy (SIMS), Auger electron spectroscopy (AES) and scanning electron microscopy (SEM) in order to fully answer them. The details and results of this study are being reported in a separate article. For the purposes of the present discussion, we present the following summary of our findings:

a)   The silver electrode surfaces which have been used to observe the anomalously high intensity Raman scattering by adsorbed pyridine have all been previously subjected to an "electrochemical roughening" procedure in which a AgCl layer is first produced during an anodic half-cycle. Upon reduction, this becomes a layer of spongy silver.

b)   All surface spectroscopies utilized indicate that chemical contamination of this surface is negligible. These findings refute the suggestion by Jeanmaire and Van Duyne that the pyridine may be complexed to adsorbed Cl^- ions.[45] More important, from a physical point of view, the image theory approach we have used is completely applicable, for reasons explained below.

c)   Examination of the surface by SEM clearly demonstrates the sponge-like nature of the surface. The field is dominated by particles of Ag that are approximately ellipsoidal or even dumbbell in shape, all more or less connected with each other. Each ellipsoid is about 200 nm × 600 nm in cross-section. In addition, there are numerous voids and channels having similar dimensions, thus affording extensive opportunity for adsorption. The packing fraction appears to be approximately 2/3 - 3/4. It is possible to "look down" the voids to depths of at most 1000 nm. This is probably an upper limit to the total thickness of the several layers. By "unfolding" the ellipsoids, the surface roughness factor is estimated to be 3 - 5 per layer, or 10 - 15 altogether.

d)   Because the diameter of each ellipsoid is so much larger than the penetration depth of 488 nm light in bulk Ag (13.2 nm), only the first layer of particles can interact with light, and the layers obscured by the first do not participate in optical processes at all.

e)   Although the total surface area may be larger than estimated earlier--and, hence, more pyridine may be adsorbed than

previously surmised--pyridine adsorbed on the obscured layers does not "see" the light, and therefore does not scatter it.

f)   Light which may reach the obscured layers by way of diffuse scattering through the channels and voids may be inelastically scattered by pyridine adsorbed to those layers, but little of this light can escape, again because the penetration depth is that of bulk Ag.

For all these reasons, the increase in surface area due to the sponge-like nature of the Ag surface cannot account for the observed enhancement of Raman intensity. Furthermore, it is of the nature of the image theory that, provided the adsorbed molecules are commonly oriented with respect to the <u>average</u> surface, the surface selection rules will still apply in the case of a sponge-like surface, just as they apparently do with supported metal catalysts.[29] The origin of the intensity enhancement is discussed in the next section.

VII. MECHANISMS FOR ENHANCEMENT OF RAMAN INTENSITY BY METAL SURFACES

Four distinct mechanisms for the role of metal surfaces in Raman scattering of adsorbed layers are conceivable. These are as follows.

1)   The first mechanism is normal Raman excitation. In this mechanism, the metal surface plays no significant role other than as a support for the molecular layer. Assuming that the layer is oriented, maximum number density would correspond to one molecule adsorbed per metal atom, or $\sim 10^{15}$ cm^{-2}. All the considerations

of Secs. II and III with respect to polarization and angle of incidence apply but, as previously noted, some gain may be expected (a factor of $\sim 10^2$) if a prism coupler is used. The intensity of Raman scattering is linear in the number density. The order-of-magnitude calculation of the previous section indicates that, to a first approximation, intensities 10^{-4} less than those of liquid samples are to be expected.

In drawing this conclusion, the absence of chemical interaction between a surface and an adsorbate (such as the pyridine complexed to adsorbed Cl^- ions postulated by Jeanmaire and Van Duyne[45]) has been implicitly assumed. This assumption is based on a theorem due to Tang and Albrecht[67] in which it is shown that if a molecular system can be partitioned, such that the wavefunction of its electronic ground state is an antisymmetrized product function of non-interacting groups, the contribution of each group to the total derived polarizability tensor component $\alpha'_{\rho\sigma}$ comes only from the relative motion of the nuclei within the ith group. Hence, to the extent that it appears as a factor in the product wavefunction, any fragment that is a simple ion cannot contribute any Raman intensity, nor can its relative motion with respect to the rest of the system. Thus, little Raman intensity should arise from the relative motion of pyridine and either adsorbed Cl^- ions or from that of pyridine and the metal substrate itself. The strong Raman line at 239 cm^{-1} in pyridine adsorbed to Ag therefore is probably not due to Ag-pyridine bond stretching.

We proceed to consider if complex formation can redistribute the intensities of Raman lines of the individual members of a complex so as to cause the apparent intensity enhancement. A similar or related phenomenon would be the redistribution of intensities of two scatterers when they are dissolved in one another. It also follows from the theorem of Tang and Albrecht that, to the extent that the wavefunction of a complex can be factored into two groups, all of $(\alpha'_{\rho\sigma})_i$ must come from the relative motion of the nuclei within each group--solute or solvent, substrate or adsorbate. Thus, only if there is evidence of major chemical change in one or the other group, such as a significant change in the vibrational frequencies of the adsorbate, could there be any additional contribution to $(\alpha'_{\rho\sigma})_i$--i.e., an intensity enhancement due to complex formation. Because the frequencies of adsorbed pyridine are so similar to those of liquid or aqueous pyridine, we conclude that the intensity enhancement observed with adsorption on Ag cannot be due to the formation of some chemical complex.

2) There has been a suggestion that enhanced Raman intensity on metal surfaces is due to the presence of high local electric fields.[45,55] However, the effects we are dealing with here (intensity enhancements by factors of $\sim 10^4$) are not small perturbations, such as those discussed by Worlock[55] and by Anastassakis et al.[68] Furthermore, the enhancement occurs at normal Raman frequencies. Hence, any electric fields responsible for this effect must be modulated at molecular frequencies,

and they must involve first order susceptibilities.[69] In other words, we are not dealing here with the hyper-Raman effect.

There is, however, a molecular analog which is helpful in understanding how electric field enhancement could occur. The collision-induced absorption spectrum of hydrogen has been shown to be the result of a quadrupole-induced dipole moment

$$\dot{P}_q = \alpha_2 \dot{E}_1 + \dot{\alpha}_1 E_2 \tag{29}$$

where molecule 1 is vibrating and molecule 2 is not, and where E and α are the quadrupole field and polarizability, respectively.[70] In the case of the interaction of a molecule with a surface, the induced dipole moment due to a local field likewise has two terms:

$$\dot{P} = \alpha_m \dot{E}_d + \dot{\alpha}_d E_m \tag{30}$$

where α_m is the polarizability of the metal, α_d is that of an adsorbed dielectric, E_d the time-dependent field caused molecular modulation, and E_m is the local field at the surface of the metal. For a dipole of 1 Debye normal to a metal surface, E_m can be estimated from image theory to be $\sim 10^6$ V cm^{-1}. If the surface is rough, however, it may be considerably larger. Judging from the work of Anastassatkis et al., however, this term is small, even for large E_m.[68] Furthermore, if this term were important, the Raman spectra of I_2 and CO on Pt should not have comparable intensity,[58,59] but should differ in intensity by

approximately one order of magnitude.[61] The first, or molecular modulation term, is the essentially that which is responsible for the Raman effect in metals,[71] since it corresponds to a change in the susceptibility induced by a phonon; in this case the phonon is furnished by the dielectric layer. The expected Raman intensity should therefore not be greater than that of metals themselves, which are not overly large.[72]

From the charge density at a point on the interface of two semi-infinite dielectrics ε_1 and ε_2 induced by a point charge situated above the interface but imbedded in ε_1, it can be shown[73] that the magnitude of an image dipole is given by

$$P_{image} = \frac{\varepsilon_2 - \varepsilon_1}{\varepsilon_1(\varepsilon_2 + \varepsilon_1)} P_{source} \tag{31}$$

For the case where $\varepsilon_1 \cong 1$ and $\varepsilon_2 = \hat{\varepsilon}$,

$$P_{image} = \frac{\hat{\varepsilon} - 1}{\hat{\varepsilon} + 1} \tag{32}$$

where $\hat{\varepsilon}$ is given by Eq. (4).

The total scattering intensity due to the source dipole plus its image is then proportional to $[1 + (\hat{\varepsilon} - 1)/(\hat{\varepsilon} + 1)]^2$. Two conclusions can be drawn from this. First, as $\omega \to 0$ the total intensity should not vary with the frequency of the exciting

light and, second, any intensity enhancement due to this induced
dipole will be minor, since the scattering <u>amplitude</u> can at most
be doubled.

3)   We have assumed throughout all of our considerations
that a metal surface plays no role in the de-excitation of an
adsorbed molecule. Measurements of fluorescence lifetimes as a
function of distance of the emitter from a metal surface have
clearly demonstrated that a metal surface does indeed offer
a non-radiative channel for the decay of electronic excitation,[74]
and two complimentary theoretical treatments have been able to
quantitatively account for these measurements.[18,19] In one of
these treatments, the dipole coupling of an excited molecule to
the non-radiative branch of a surface plasmon is the basis of
the decay channel. We remark again in passing that surface rough-
ness, which is provided by the adsorbed molecule itself, is a
necessary condition for this coupling.

Assuming that the dipolar coupling is measured by a "golden
rule"

$$\Gamma \sim \frac{2\pi}{\hbar} \left| H_{mn} \right|^2 D(\omega) \tag{33}$$

where $D(\omega)$ is the density of surface plasmons, we may expect the
coupling to be greatest in the vicinity of ω_{sp}, since the density

function which is given by[18]

$$D(\omega) = \frac{\omega}{2\pi c^2} \frac{(1 + \varepsilon^2)}{(1 + \varepsilon)^2} \tag{34}$$

is singular there. Substitution of Eq. (4) into Eq. (34) shows that $D(\omega)$ closely resembles the frequency distribution function of a one-dimensional monatomic crystal. As $\omega \to 0$, $D(\omega)$ is linear in ω, but as $\omega \to \omega_{sp} = \omega_p/\sqrt{2}$, the dominant term in $D(\omega)$ varies as $(2\omega^2 - \omega_p^2)^{-\frac{1}{2}}$.[75]

In the other treatment, the classical dipole-dipole coupling of an electronic transition of a molecule with that of its image is calculated.[19] Here too, for a metal whose dielectric function is given by Eq. (4), the coupling becomes resonant at $\omega = \omega_{sp}$.

Since an electronic excitation may decay to a surface plasmon,[18,19] we should also consider the reverse process as a possible mode of excitation of an adsorbed molecule. The individual steps of this excitation process are thus envisaged as:

(a) Light excites the non-radiative surface plasmon branch, aided by the surface roughness.

(b) The surface excitation wave, now radiative, excites the molecular electronic transition.

According to this model, the coupling parameter is given by Eq. (33). The only way for this process to yield larger scattering intensities than those of the normal Raman effect is for the overall matrix element H_{mn} for steps (a) and (b) to be larger than that for ordinary Raman scattering. The latter is

by definition of second order, but more important, the contribution of step (a) to $|H_{mn}|^2$ is proportional to the extinction coefficient of the metal, which is large in the region $\omega < \omega_{sp}$. Furthermore, as $\omega \to 0$, the extinction coefficient increases approximately as ω^{-1}. Since in this region $D(\omega)$ is linear in ω, the intensity of scattered radiation should not vary with the excitation frequency ω.

4) Philpott has also raised the possibility that, due to the coupling of the molecular states with surface plasmons, adsorbed molecules may manifest the resonance Raman effect at excitation frequencies which would otherwise give rise to only the normal Raman effect.[18] The fact that the intensities of particular modes are primarily enhanced strongly suggests a resonance effect. There are two ways resonance Raman enhancement can come about:

(a) As shown by Jacon and coworkers using a Greens function formalism, Raman scattering which involves discrete intermediate states has differential intensity given by

$$\frac{dI_{ab}}{d\Omega} = \frac{I_o}{c^4} (\omega_o + \omega_{ab})^4 \left| \frac{i\pi}{\hbar} \sum_r \frac{\langle b|H_{int}|r\rangle\langle r|H_{int}|a\rangle}{E_r + \Delta_r - E_a - \hbar\omega_o - i\Gamma_r/2} \right|^2 \quad (35)$$

where Γ_r is the width and Δ_r is the Lamb shift of the intermediate state, $|r\rangle$.[76] In the gas phase, where Γ_r is the radiative width of the rth level, there will be at least one term in this sum which becomes singular as $\omega_o \to \omega_{ra}$. For an adsorbed molecule, just as for one involved in a collision with another molecule,

Γ_r has both radiative and non-radiative components. It is then possible that Γ_{sp}, the width contributed by coupling to the surface plasmons, may make the scattering become resonant at a different frequency than ω_{ra}.

(b) If the intermediate state or states $|r>$ are in the continuum, however, the scattering tensor assumes a different form. When $|r>$ is discrete, provided $\hbar\omega_o >> E_r - E_a$, the width Γ_r can be neglected. If $|r>$ is in the continuum, however, this is not possible, for the sum over r will diverge near $E_r - E_a - \hbar\omega_o$. In order to evaluate the scattering tensor, an infinitesimal $i\varepsilon$ is added to the "resonance denominator," and use is made of a property of the δ-function, namely that

$$\lim_{\varepsilon \to +0} \frac{1}{x - x_o + i\varepsilon} = P \frac{1}{x - x_o} - i\pi\delta(x - x_o) \tag{36}$$

where P indicates the principal value. Applying this integral identity, Jacon et al. have shown that the differential intensity becomes[77]

$$\frac{dI_{ab}}{d\Omega} = \frac{I_o}{c^4} (\omega_o + \omega_{ab})^4 \left| \frac{i\pi}{h} [<b|H_{int}|\alpha><\alpha|H_{int}|a>\rho_\alpha(\omega')]_{\omega' = \omega_o} \right.$$

$$\left. + P \int_{continuum} \frac{<b|H_{int}|\alpha><\alpha|H_{int}|a>}{\hbar(\omega' - \omega_a - \omega_o)} \rho_\alpha(\omega')d\omega' \right|^2 \tag{37}$$

where $\hbar\omega$ is the energy of state $|\alpha>$ of the continuum. Model calculations of Raman intensities in the Born-Oppenheimer approximation have shown that the first, or resonant, term in this sum is

not necessarily the most important.[78] The principal part of the integral can be the major term provided absorption into the continuum is unsymmetrical with respect to the excitation wavelength (and, as we shall see, this is probably the case here).

Resonance Raman intensity then depends on not just one precise resonance $\omega_o = \omega_{ra}$, but all intermediate states $|\alpha>$ make a contribution, weighted by the density of states, $\rho_\alpha(\omega')$. The continuum states $|\alpha>$ are eigenstates of the Hamiltonian $H_o + V_r$, where H_o is the Hamiltonian of the free molecule, and V represents the electromagnetic field. Eq. (37) is exact and is not the result of the application of first-order perturbation theory, in which V is taken as a small perturbation. In other words, $|\alpha>$ is a state of the system, molecule + field.

The interaction of interest to us, however, is of the molecular states $|a>$, $|b>$, $|r>$, etc., with the surface plasmons $|k>$ which, as we have seen, are light-like. There is therefore a new set of states which form a continuum--the entire band of surface plasma states $\omega \leq \omega_p$. The scattering tensor displayed in Eq. (37) may then account for the resonant-like scattering observed with metal surfaces.

Substitution of Eq. (34) in Eq. (37) (principal part) gives the dependence of the scattered intensity on the exciting frequency, ω_o. Since we are interested only in the intensity enhancement due to the interaction with the surface plasma states, the $I_o(\omega_o + \omega_{ab})^4 c^{-4}$ term has been suppressed. The _relative_ intensity

is then given by

$$I(\omega)_{rel} \sim \left[P \int_{band} \frac{|H_{int}(\omega)|^2 \omega (1 + \varepsilon^2)(1 + \varepsilon)^{-2} d\omega}{2\pi c^2 \hbar (\omega - \omega_a - \omega_o)} \right]^2 \tag{38}$$

Using Eq. (4) this can also be written as

$$I(\omega)_{rel} \sim \left[P \int_{band} \frac{\omega |H_{int}(\omega)|^2}{2\pi c^2 \hbar (\omega - \omega_a - \omega_o)} \left\{ \frac{\omega^2 - \omega_p}{2\omega^2 - \omega_p^2} + \frac{\omega_p^2 \omega^2}{(2\omega^2 - \omega_p^2)^2} \right\} d\omega \right]^2 \tag{39}$$

In order to calculate the quantitative intensity enhancement upon adsorption, the actual $H_{int}(\omega)$ would have to be known. Since we know only its approximate frequency dependence, we can only find that of the _relative_ intensity $I(\omega)$. As $\omega \to 0$, the term in braces approaches unity and, as noted earlier, $|H_{int}(\omega)|^2$ increases as ω^{-1}. Under these circumstances, the dependence of the _relative_ scattered intensity on the exciting frequency ω_o is given by

$$I(\omega)_{rel} \sim \left[P \int_0^{\omega_p} \frac{d\omega}{\omega - \omega_o} \right]^2 = [\ln(y - 1)]^2 \tag{40}$$

where $y = \omega_p / \omega_o$. Thus, the _relative_ scattered intensity of an adsorbed layer should increase logarithmically with decreasing frequency.

Interaction of a discrete state with a continuum thus creates an entire new set of states, and the scattered intensity calculated by Eq. (37) involves all of them, weighted by the density of states. The additional intensity derives from the contribution of the entire band. As already noted, the modulus of the matrix element

H_{int} is relatively large in the frequency region of interest
$(\omega < \omega_p)$. Even so, as with all mixings of states, total inten-
sity is conserved.

The resonance of a discrete state with a continuum, which is
the basis of Eq. (37), is encountered in a number of related
problems, such as autoionization[79] and Fermi resonance in molecular
crystals.[80] The common feature of these problems is that the
coefficient which measures the weight of the discrete state in
the continuum-plus-discrete state mixture undergoes a sharp vari-
ation at or near the resonance, so that the scattered intensity
is still peaked there. The effect of Eq. (37) is therefore to
enhance the Raman scattering at the resonance by contributions
from the entire band, peaking the intensity at that point. The
total integrated intensity is not changed, but at the resonance
the contributions gained from the interactions $<a|H_{int}|\alpha>$ through-
out the band make their appearance.

The Raman spectrum of pyridine adsorbed on an Ag electrode
has been measured using as many as seven different laser lines
for its excitation.[81] The intensity of the 1026 cm^{-1} Raman line
of adsorbed pyridine, measured relative to the corresponding line
of liquid pyridine (991 cm^{-1}), when plotted versus the frequency
of the exciting light (λ 457.9, 465.8, 476.5, 488.0, 514.5 and
632.8 nm) indicates a dependence on that frequency approximately
of the form $I_{rel} \sim k\omega^{-2}$. This excludes the simple dipole coupling
model, but it is not very different from the form of Eq. (40). We

are presently carrying out a careful study of the frequency depen-
dence with a 1W cw dye laser in order to accurately determine the
power law.

VIII. SUMMARY

It has been our purpose in this article to discuss the
selection rules and relative intensities of Raman spectra of
molecules adsorbed to metal surfaces. Our starting point has
been that such surfaces are not passive, but play an active role
in the spectroscopy. We have therefore reviewed surface excita-
tions of metals (i.e., surface plasmons), and the ways in which
light can be coupled to these excitations. Because we are
generally interested in the reflective region of the metals
($\frac{1}{\tau} < \omega < \omega_p$), we have concentrated on the normally non-radiative
branch of the surface plasmon dispersion curve.

Following this, we have discussed the optimization of inci-
dence and scattering angles for Raman spectroscopy of metal
surfaces, as well as polarization and analysis directions. In
distinction from infrared reflection-absorption experiments, as
a result of the optical constants of metals and dielectric over-
layers in the visible region of the spectrum, it is found that
angles of incidence do not have to be glancing, and useful infor-
mation can be obtained with either TE or TM (s or p) polarization.

The image field model of Pearce and Sheppard for selection
rules for infrared reflection-absorption spectra of metal surfaces[27]
is then re-examined. It was found that this model can be expressed

in group theoretical terms. The activity representations of
an adsorbed molecule, for both infrared and Raman spectroscopy,
are those of the direct product group $\underset{\sim}{M} = \underset{\sim}{G} \otimes \{\underline{E} + \underline{R}\}$, where $\underset{\sim}{G}$
is the point group of the molecule, and $\underline{R}$ is the combined or
simultaneous operation $\underline{R} = \sigma_h \underline{C}$ ($\underline{C}$ = change conjugation). Among
the spectroscopic consequences of this new group is the ability
to detect molecular orientation on a metal surface, provided the
molecules are commonly oriented. Some of these consequences are
also valid for insulating surfaces, under circumstances we have
discussed at the end of Sec. IV.

As expected, the analysis of Raman spectra of ordered mono-
layers has a number of similarities to that of three-dimensional
crystals. Some of these are also discussed in Sec. IV, but their
chief value has been in defining particular $\underline{i}(\underline{pa})\underline{s}$ geometries[43]
in order to obtain meaningful depolarization values. In some
cases, different molecular orientations can be distinguished using
the experimental depolarization factors.

In Sec. VI, a number of recent spectroscopic studies of
metal surfaces are discussed, including some which have utilized
the relatively new techniques of ELS and IETS. This discussion
is chiefly aimed at testing the validity of the metal surface selec-
tion rules described above. Also in this section the Raman
scattering measurements which have been carried out to date are
reviewed, especially those of pyridine on silver, and the basis
of the claims that the intensity of this spectrum is enhanced by

four (or more) orders of magnitude is carefully analyzed. Our conclusion is that the enhancement factor is $\sim 10^4$. Then the results of our own examination of this surface using several particle surface spectroscopies are summarized. From this summary we conclude that the enhancement cannot be the result of either chemical contamination of the surface or of extraordinary surface roughening.

Finally, four physical theories for the intensity enhancement are discussed, both from the point of view of the intensity enhancement each may cause, and in addition the dependence of the _relative_ intensity on the frequency of the light used to excite the Raman spectrum. It is concluded that the enhancement is most likely a resonance Raman effect in which the surface plasmons mix with molecular electronic states so as to form a continuum of intermediate states for the scattering. Thus, the availability and accessibility of a metal's conduction electrons is of essential importance in the enhancement of the Raman activity of that which is adsorbed to the surface of the metal.

IX. ACKNOWLEDGMENTS

References

1. N. G. Yaroslavskii and A. N. Terenin, Doklady Acad. Nauk. S. S. S. R. 66, 885 (1949).

2. J. E. Mapes and R. G. Eischens, J. Phys. Chem. 58, 1049 (1954).

3. G. W. Greeneles, et. al., Cpt. Comm. 23, 236 (1977).

4. R. G. Greenler and T. L. Slager, Spectrochim. Acta 29A, 193 (1973).

5. R. G. Greenler, J. Chem. Phys. 44, 310 (1966).

6. J. D. E. McIntyre and D. E. Aspens, Surface Sci. 24, 417 (1971). See also J. D. E. McIntyre in Optical Properties of Solids-- New Developments, B. O. Seraphin, ed. (American Elsevier Publishing Co., New York (1976) p. 555.

7. F. Wooten, Optical Properties of Solids, (Academic Press, New York, 1972).

8. J. C. Decius and R. M. Hexter, Molecular Vibrations in Crystals (McGraw-Hill, 1977) Sections 4-8 and 5-7.

9. F. Abeles, Physics of Thin Films 6, 151 (1971). See also R. A. Ferrell, Phys. Rev. 111, 1214 (1958).

10. A. J. McAlister and E. A. Stern, Phys. Rev. 132, 1599 (1963). See also D. Schulz and M. Zurheide, Z. Phys. 211, 165 (1968).

11. H. Raether, Physics of Thin Films 9, 145 (1977).

12. S. A. Rice, et al., Advances in Chemical Physics 27, 543 (1974).

13. Y.-Y. Teng and E. A. Stern, Phys. Rev. Lett. 19, 511 (1967).

14. D. Beaglehole, Phys. Rev. Lett. 22, 708 (1969).

15. I. Pockrand, J. Phys. D9, 2423 (1976).

16. H. Raether, Nuovo Cimento 39B, 817 (1977).

17. A. Otto in Optical Properties of Solids New Developments, B. O. Seraphin, ed. (American Elsevier Publishing Co., New York, 1976) p. 677.

18. M. R. Philpott, J. Chem. Phys 62, 1812 (1975). See also H. Morawitz and M. R. Philpott, Phys. Rev. 10B, 4863(1974).

19. R. R. Chance, A. Prock and R. Silbey, J. Chem. Phys. 62, 2245 (1975).

20. P. Drude, The Theory of Optics, C. R. Mann and R. A. Millikan, transl. (Longmans, Green and Co., London, 1920) p. 287.

21. O. S. Heavens, <u>Optical</u> <u>Properties</u> <u>of</u> <u>Thin</u> <u>Solid</u> <u>Films</u> (Butter-worths, London, 1955) p. 54.

22. J. D. E. McIntyre in <u>Optical</u> <u>Properties</u> <u>of</u> <u>Solids</u> <u>New</u> <u>Develop-ments</u>, B. O. Seraphin, ed. (American Elsevier Pub'ishing Co., New York, 1976) Chapter 11.

23. $\hat{n}_i = n_i - ik_i$, and ϱ_i is the complex angle of the incidence in phase i.

24. M. J. Dignam, M. Moskovits and R. W. Stobie, Trans. Faraday Soc. <u>67</u>, 3306 (1971).

25. D. W. Berreman, Phys. Rev. <u>130</u>, 2193 (1963).

26. H. Ibach, Surface Sci. <u>66</u>, 56 (1977).

27. M. Dignam, B. Rao and J. Moskovits, J. Chem. Soc., Faraday II <u>69</u>, 804 (1973). In this article the authors gave a similar interpretation to some of the results of Ref. 24.

28. S. A. Francis and A. H. Ellison, J. Opt. Soc. Am. <u>49</u>, 131 (1959).

29. H. S. Pearce and H. Sheppard, Surface Science <u>59</u>, 205 (1976).

30. H. Ibach, M. Hopster and B. Sexton, Appl. Surf. Sci. <u>1</u>, 1 (1977).

31. The possibility of effects due to "partial imaging" was mentioned but not pursued in Ref. 27.

32. E. B. Wilson, J. C. Decius and P. C. Cross, <u>Molecular</u> <u>Vibra-tions</u>, (McGraw-Hill Book Co., 1955).

33. J. C. Decius and R. M. Hexter, <u>Molecular</u> <u>Vibrations</u> <u>in</u> <u>Crystals</u>, (McGraw-Hill, 1977), Sec. 5-6 and Sec. 6-3(f).

34. See Reference 32, Sec. 3-6.

35. C. J. Bradley and A. P. Cracknell, "The Mathematical Theory of Symmetry in Solids," (Oxford, 1972), p. 570.

36. A. P. Cracknell, Thin Solid Films <u>21</u>, 107 (1974).

37. A. P. Cracknell, Thin Solid Films <u>24</u>, 279 (1974).

38. N. V. Belov, Sov. Phys. Crystall. <u>4</u>, 775 (1959); a few minor errors have been corrected.

39. Reference 33, Sec. 4-4.

40. The simple construction used to demonstrate the metal surface selection rule is also valid for all $k \neq 0$.
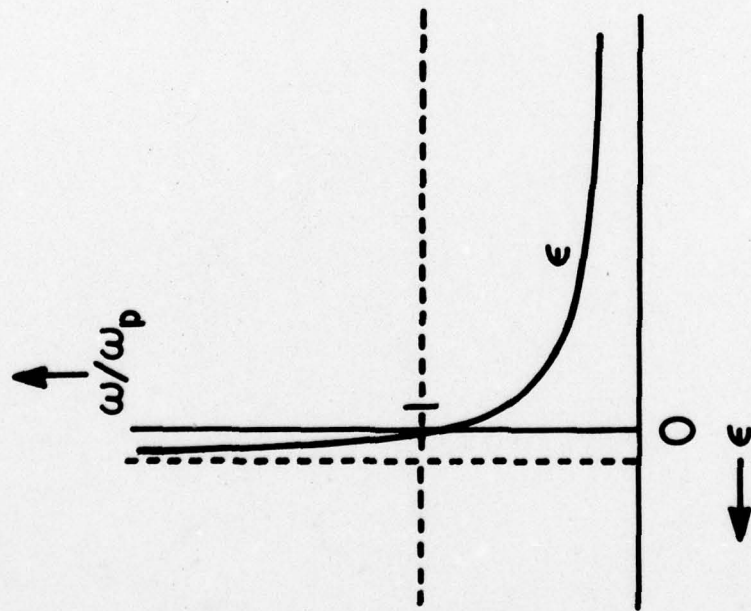
41. Y. J. Chen, W. P. Chen and E. Burstein, Phys. Rev. Lett. $\underline{36}$, 1207 (1976).

42. Reference 33, Appendix X.

43. Reference 33, p. 169.

44. One of these cases (Scattering geometry 2, Case $\underline{ii}$) is related to an example discussed by Jeanmaire and Van Duyne.[45] These authors discussed the case of Raman scattering by a molecule lying flat on the surface of a metal electrode, using normal incidence excitation, and correctly concluded that under these circumstances $\rho_\ell = 0$. For an axially-attached molecule (Case $\underline{i}$), with no restrictions of the incident radiation, the same authors calculate a depolarization ratio of $\frac{1}{2}$ by an approximate technique. The correct value, using Snyder's procedure[46] is $(\underline{a} - \underline{b})^2/[2(\underline{a} + \underline{b})^2 + (\underline{a} - \underline{b})^2]$.

45. D. L. Jeanmaire and R. P. Van Duyne, J. Electroanal. Chem. $\underline{84}$, 1 (1977).

46. R. G. Snyder, J. Molec. Spectry. $\underline{37}$, 353 (1971).

47. E. Evans and D. L. Mills, Phys. Rev. $\underline{B5}$, 4126 (1972).

48. J. E. Demuth and D. E. Eastman, Phys. Rev. Lett. $\underline{32}$, 1123 (1974).

49. D. J. Scalapino and S. M. Marcus, Phys. Rev. Lett. $\underline{18}$ 459 (1967).

50. J. Lambde and R. C. Jaklevic, Phys. Rev. $\underline{165}$, 821 (1968).

51. M. G. Simonsen, R. V. Coleman and P. K. Hansma, J. Chem. Phys. $\underline{61}$, 3789 (1974).

52. J. Kirtley, D. J. Scalapino and P. K. Hansma, Phys. Rev. $\underline{14B}$, 3177 (1976).

53. J. Kirtley and P. K. Hansma, Surface Sci. $\underline{66}$, 125 (1977).

54. A. Pinczuk and E. Burstein, Phys. Rev. Lett. $\underline{21}$, 1073 (1968). See also in Intl. Conf. on Light Scattering Spectra of Solids, New York University, G. B. Wright, ed. (Springer-Verlag, Berlin, 1969), p. 429.

55. J. M. Worlock, Intl. Conf. on Light Scattering Spectra of Solids, New York University, G. B. Wright, ed. (Springer-Verlag, Berlin, 1969), p. 411.

56. Y. J. Chen, W. P. Chen and E. Burstein, Bull. Am. Phys. Soc. $\underline{21}$, 338 (1976). See also Intl. Conf. on Light Scattering in Solids, Campinas, Brazil, 1975, M. Balkanski, R. C. C. Leite and S. P. S. Port, eds. Flammarion, Paris, (1976), p. 525.

57. Y. J. Chen, W. P. Chen and E. Burstein, Phys. Rev. Lett. $\underline{36}$, 1207 (1976).

58. R. P. Cooney, E. S. Reid, P. J. Hendra and M. Fleischmann, J. Am. Chem. Soc. $\underline{99}$, 2002 (1977).

59. R. P. Cooney, M. Fleischmann and P. J. Hendra, J. C. S. Chem. Comm. 1977, 235.

60. R. P. Cooney, E. S. Reid, M. Fleischmann and P. J. Hendra, J. C. S. Faraday I $\underline{73}$, 1691 (1977).

61. T. V. Long and R. A. Plane, J. Chem. Phys. $\underline{43}$, 457 (1965).

62. A. J. McQuillan, P. J. Hendra and M. Fleischmann, J. Electroanal. Chem. $\underline{65}$, 933 (1975).

63. M. G. Albrecht and J. A. Creighton, J. Am. Chem. Soc. $\underline{99}$, 5215 (1977).

64. J. J. Barrett and N. I. Adams III, J. Opt. Soc. Am. $\underline{58}$, 311 (1968).

65. R. G. Barradas and B. E. Conway, J. Electroanal. Chem. $\underline{6}$, 314 (1963).

66. M. G. Albrecht and R. M. Hexter, to be published.

67. J. Tang and A. C. Albrecht, J. Chem. Phys. $\underline{49}$, 1144 (1968).

68. E. Anastassakis, A. Filler and E. Burstein, Intl. Conf. on Light Scattering in Solids, New York University, 1969, G. B. Wright, ed. (Springer-Verlag, Berlin, 1969), p. 421. See also Phys. Rev. $\underline{2B}$, 1952 (1970).

69. M. Cardona, Surface Sci. $\underline{37}$, 100 (1973).

70. F. R. Britton and M. F. Crawford, C. J. Phys. $\underline{36}$, 761 (1958).

71. D. L. Mills, A. A. Maradudin and E. Burstein, Intl. Conf. on Light Scattering in Solids, New York University, 1969, G. B. Wright, ed. (Springer-Verlag, Berlin, 1969), p. 399.

72. J. H. Parker, D. W. Feldman and M. Ashkin, J. Chem. Phys. $\underline{49}$, 1144 (1968).

73. J. D. Jackson, Classical Electrodynamics (Wiley, New York, 1962), p. 110.

74. H. Kuhn, J. Chem. Phys. $\underline{53}$, 101 (1970); K. H. Drexhage, Progress in Optics $\underline{12}$, 165 (1974).
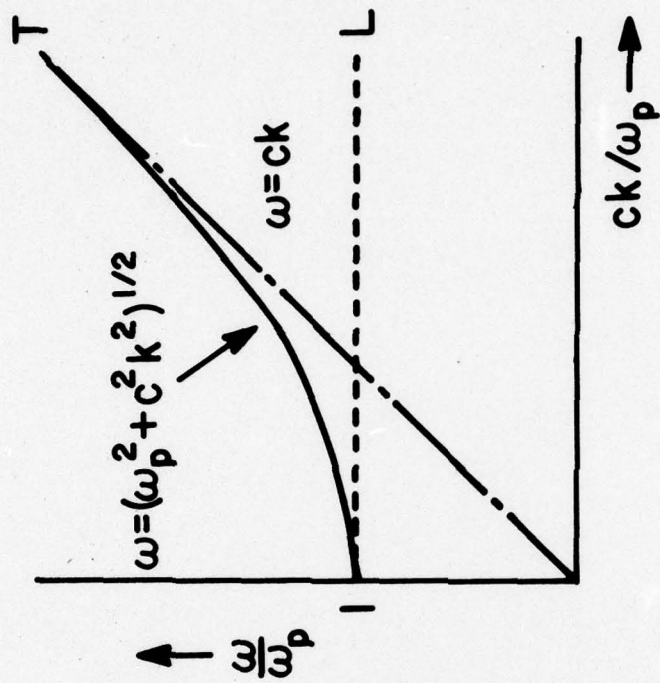
75. The linear dependence of $D(\omega)$ on ω as $\omega \to 0$ can be shown by straightforward differentiation of Eq. (8), followed by the use of Eq. (4) for ε_1 and an examination of the variation of $D(\omega)$ with the reduced frequency $\omega/\omega_p \to 0$. The result also demonstrates how $D(\omega)$ resembles the frequency distribution function $g(\omega)$ of a two-dimensional monatomic crystal, because in ℓ dimensions, as $\omega \to 0$, $g(\omega) \sim \omega^{\ell-1}$, as proven by L. Van Hove, Phys. Rev. $\underline{89}$, 1189 (1953).

76. M. Jacon, Advances in Raman Spectroscopy, Volume 1 (Proc. Third Intl. Conf. on Raman Spectroscopy, Reims, 1972), J. P. Mathieu, ed. (Heyden & Son, Ltd., London, 1973), p. 325. There is a similar term involving $E_r - E_b + \hbar\omega_0$ which arises when the intermediate state is reached by the creation of the photon $\hbar\omega_0$.

77. M. Jacon, M. Berjot and L. Bernard, Compt. rend. $\underline{273B}$, 585 (1971).

78. M. Berjot, M. Jacon and L. Bernard, Opt. Commun. $\underline{4}$, 246 (1971).

79. U. Fano, Phys. Rev. $\underline{124}$, 1866 (1961).

80. V. M. Agranovich and I. I. Lalov, Soviet Phys. Solid State $\underline{13}$, 859 (1971).

81. J. A. Creighton, private communication.

Figure Captions
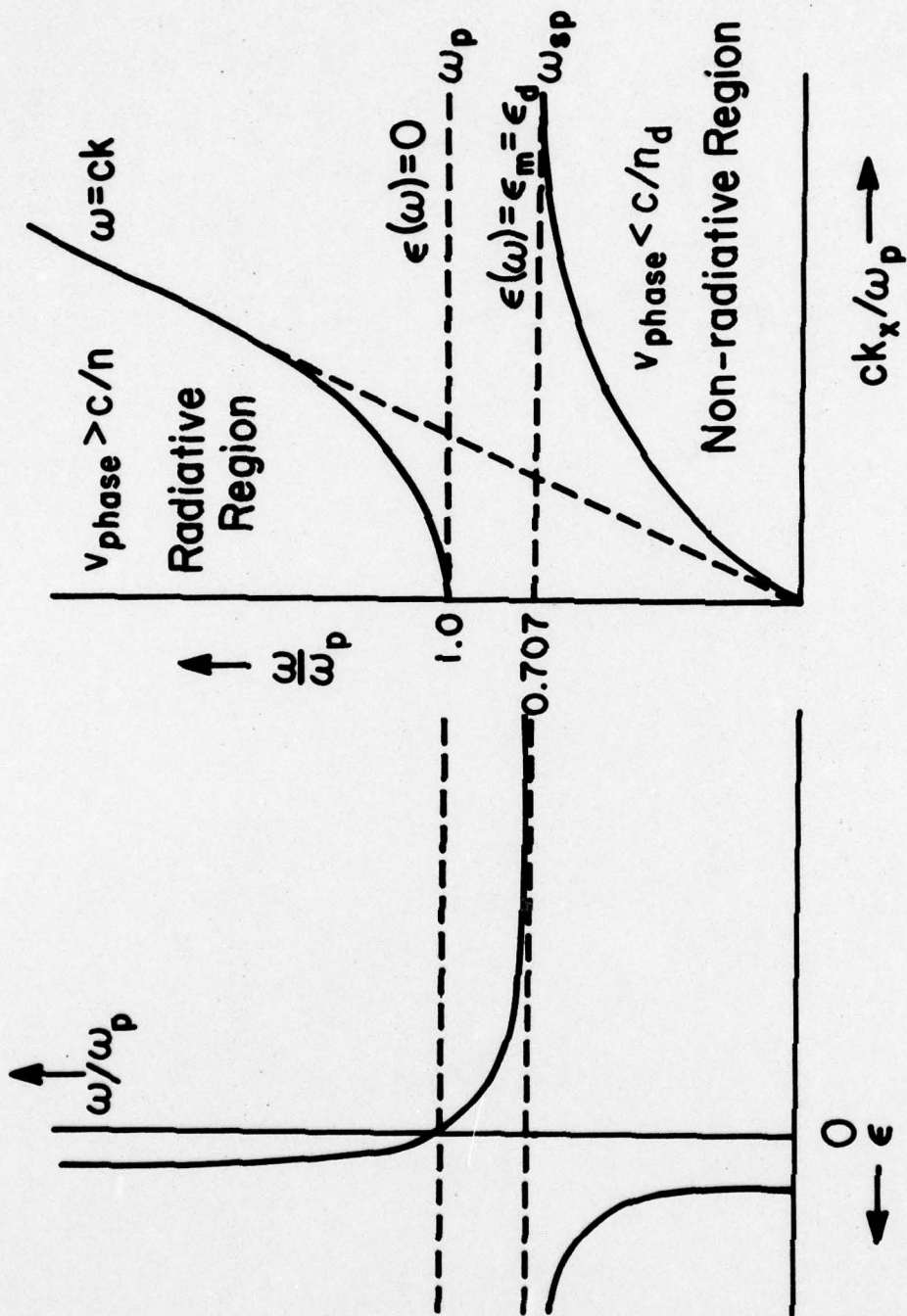
Fig. 1   Dielectric function (a) and dispersion relation (b) of a free electron metal.

Fig. 2   Dielectric function (a) and dispersion relation (b) of a two-phase system, dielectric and metal.

Fig. 3   Prism coupling of evanescent wave of two-phase system, dielectric with index of refraction n_d and metal with dielectric function ε_m. The prism has index of refraction n_p.

Fig. 4   Dispersion relations of a two-phase system, dielectric and metal, due to prism coupling.

Fig. 5   Symmetric combination of a $k = 0$ vibrational mode of a linear array of source molecules and its image.

Fig. 6   Two scattering geometries using oblique incidence and TM polarization.

    (a) Scattered light viewed on surface edge

    (b) Scattered light viewed near specular angle

$\omega = (\omega_p^2 + c^2 k^2)^{1/2}$

$\omega = ck$

T

L

$\dfrac{\omega}{\omega_p}$

ck/ω_p

(b)

ω/ω_p

ϵ

O

ϵ

(a)

(a)

(b)

(a)

(b)

s=X

Y−Z

Y+Z

Z

X

X

Y

X

p=Y+Z

i=Y−Z

s=Y+Z

Y−Z

Y−Z